

COMPARISON OF A COVERED COLLECTOR  
TO AN UNCOVERED COLLECTOR FOR NOCTURNAL  
SKY RADIATION

by

DO-YOUNG HAN

B.S., Seoul National University, Seoul, Korea, 1972

---

A MASTER'S THESIS

submitted in partial fulfillment of the  
requirements for the degree

MASTER OF SCIENCE

Department of Mechanical Engineering

KANSAS STATE UNIVERSITY  
Manhattan, Kansas

1977

Approved by:

  
Major Professor

Document  
LD  
2668  
T4  
1977  
H348  
C.2

## TABLE OF CONTENTS

Chapter	Page
I. INTRODUCTION . . . . .	1
II. REVIEW OF THE LITERATURE . . . . .	3
The Properties of Tedlar . . . . .	3
The magnitude of Night Sky Radiation . . . . .	6
Practical Use of Night Sky Radiation . . . . .	10
III. THE MODEL . . . . .	11
General Considerations . . . . .	11
Radiator without Cover . . . . .	14
Radiator with Cover . . . . .	16
IV. EXPERIMENTAL WORK . . . . .	22
General Description of Test Facility . . . . .	22
Test Collectors . . . . .	22
Water Supply System . . . . .	27
Instrumentation . . . . .	27
Testing Procedure . . . . .	28
V. RESULTS AND DISCUSSION . . . . .	30
Experimental Results . . . . .	30
Comparison between Actual and Calculated Performance . . . . .	38
VI. SUMMARY, CONCLUSIONS, AND RECOMMENDATIONS . . . . .	48
Summary and Conclusions . . . . .	48
Recommendations for Further Studies . . . . .	49
SELECTED BIBLIOGRAPHY . . . . .	50
APPENDIX A NOMENCLATURE . . . . .	53
APPENDIX B COMPUTER PROGRAM . . . . .	55
APPENDIX C CALCULATED RESULTS . . . . .	59
APPENDIX D CALCULATED RESULTS . . . . .	62
APPENDIX E ERROR AND UNCERTAINTY ESTIMATION . . . . .	66

## LIST OF TABLES

Table	Page
1. Operating Conditions . . . . .	31
2. Several Values Used in Calculation . . . . .	39
3. Input Data of Run-1 and Run-2 for 6 August 1977 . . . . .	42
4. Input Data of Run-1, Run-2 and Run-3 for 2 0'clock Every Day . . . . .	46

## LIST OF FIGURES

Figure	Page
1. Transmittance of Tedlar at Short Wave Length Spectrum . . . . .	4
2. Transmittance of Tedlar at Long Wave Length Spectrum . . . . .	5
3. Typical Apparent Emissivity $\epsilon_a$ of a Clear Sky at Sea Level . . .	8
4. Typical Values of Nocturnal Sky Radiation for Clear Skies at Sea Level . . . . .	9
5. Energy Balance on the Plate . . . . .	12
6. Thermal Network for Bare Flat-Plate Radiator . . . . .	15
7. Equivalent Thermal Network for Bare Flat-Plate Radiator . . . .	15
8. Thermal Network for Covered Flat-Plate Radiator . . . . .	17
9. Equivalent Thermal Network for Covered Flat-Plate Radiator . . .	17
10. Schematic Diagram of the Test Apparatus . . . . .	23
11. A Schematic Diagram for Collector . . . . .	24
12. Construction Details of the Collector . . . . .	26
13. Flow Pattern Through Radiator and Location of Thermocouples . .	26
14. Actual Outlet Temperature at A Normal Night . . . . .	33
15. Actual Outlet Temperature at A Normal Night . . . . .	34
16. Actual Outlet Temperature at A Normal Night . . . . .	35
17. Actual Outlet Temperature at A Rainy Night . . . . .	36
18. Comparison between Actual and Calculated Outlet Temperature . .	44



## CHAPTER I

### INTRODUCTION

Air-conditioning systems using nocturnal sky radiation have received considerable attention in both the research and the engineering fields (1). Research on this topic and the development of appropriate methods of analysis have been some of the most interesting areas of solar energy activity.

Over the past fifty years, nocturnal radiant heat transfer has been shown to be an effective method for passive or active cooling of occupied spaces. Bliss (2), Brunt (3), Picha and Villanueva (4), and others (5,6) have studied the magnitude of the net outgoing thermal radiation from surfaces located on the earth. They found values of the nocturnal sky radiation to a clear sky during summer ranging from 60 watt/meter<sup>2</sup> to 100 watt/meter<sup>2</sup> (7-9). Practically, Thomason (10,11), Bliss (12), and others (13-15) demonstrated that night sky radiation can provide at least a portion of space cooling. Especially, as a active system, nocturnal radiation cooling has had its usefulness proven at an experimental Skytherm building in Phoenix, Arizona (16).

As stated above, systems relying on nocturnal sky radiation have proven to be successful for certain locations and meteorological conditions. However, in other geographical locations nocturnal radiant cooling does not prove feasible for 100% of the cooling demands because the radiator area requirements are excessive. This would not preclude nocturnally cooled water, stored for daytime use, from providing a portion of the cooling requirements. As one method nocturnal sky radiation can be used to augment solar cooling with a solar powered absorption unit which is presently commercially available.

Glass or plastic covered flat plate absorbers, which operate at the relatively low temperature, are generally used as the heat collectors in practical applications. However, with regard to the use of heat collectors for nocturnal cooling, a collector designed for heat collection is generally a poor device because of poor transmittance of its cover at long wave length spectrum. The two functions tend to work against each other (17).

Tedlar<sup>\*</sup> has special properties which may make it suitable as a cover material for both purposes. Compared with other cover materials, Tedlar is very transparent at the long and short wave length spectrums. Higher transmittance at long wave length makes the Tedlar covered collector a good radiator at night, but a poor collector at day because of its increased reradiation thermal loss. However, this thermal loss can be compensated for by the improved solar transmittance of Tedlar (18-20). Therefore, Tedlar is a good compromise material for use in nocturnal radiation as well as daytime absorption.

The objective of the present study was to compare a Tedlar covered collector with an uncovered collector when used for night sky radiation.

\*Tedlar is a Du Point registered trademark for its P.V.F. film.

## CHAPTER II

### REVIEW OF THE LITERATURE

The flat plate collector has for many years been the most popular device to collect solar heat at modest temperature. It has been used, almost to the exclusion of other devices, for the heating of domestic water. It is the most frequently considered device for use in the heating or cooling of buildings with solar energy or night sky radiation. It has been coupled to heat engines and other devices in hundreds of published hardware and theoretical studies. A thorough review of the literature and history of flat plate collector was published by Winter (21).

The literature review of this investigation is divided into three parts, namely, a literature survey on the properties of Tedlar, the magnitude of night sky radiation, and practical use of nocturnal sky radiation.

#### The Properties of Tedlar

Tedlar is a good cover material during day and night compared with glass because of its higher transmissivity at the long and short wave length spectrum. Whillier (18-20) made a numerical comparison of the heat loss coefficient between a Tedlar covered collector and a glass covered collector during day time. He showed that the heat loss coefficient of a Tedlar covered collector due to its higher transmittance of the longwave length radiation was only 15 to 20 percent greater than that of a glass covered collector. However, higher loss of Tedlar covered collector could be more or less compensated by its improved transmittance of the short wave radiation, i.e. solar radiation. In summary, he concluded that

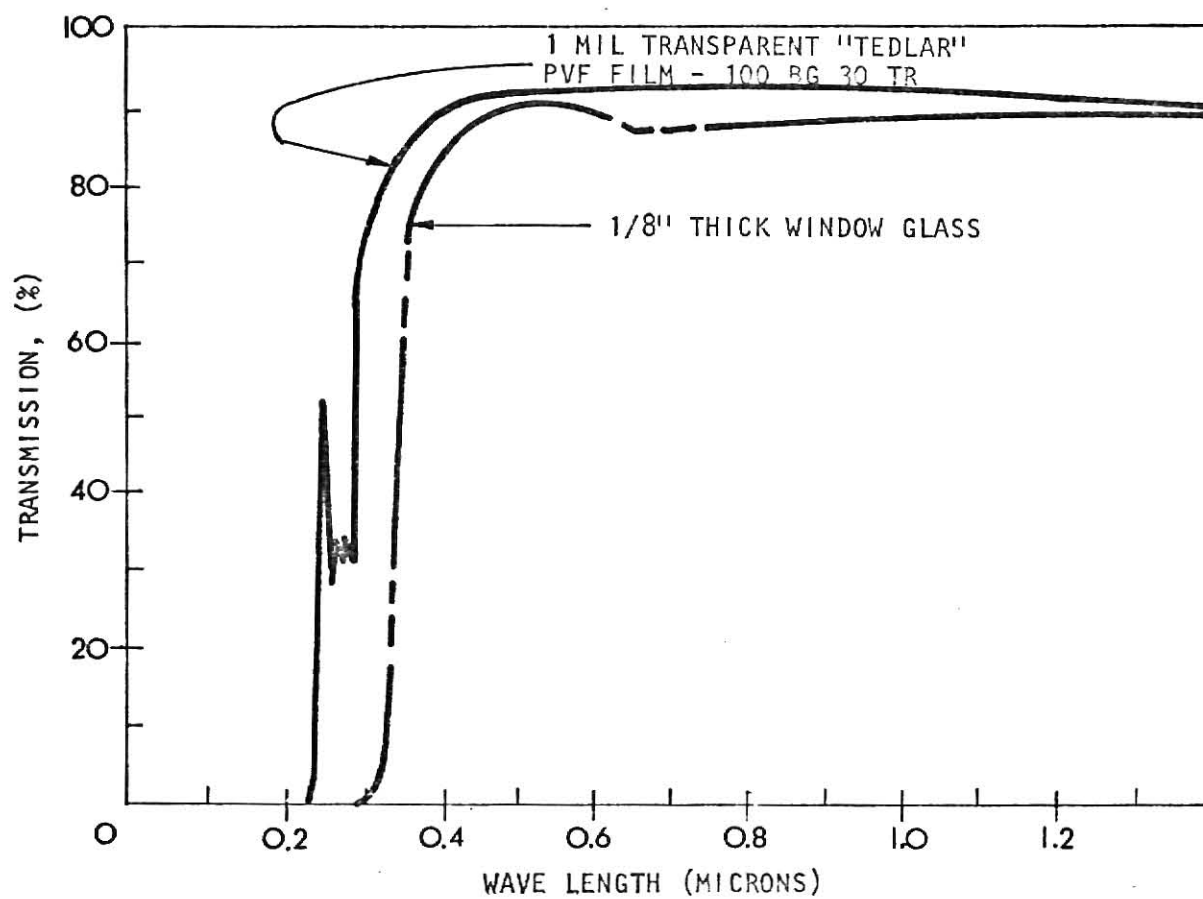


Figure 1. Transmittance of Tedlar at Short Wave Length Spectrum

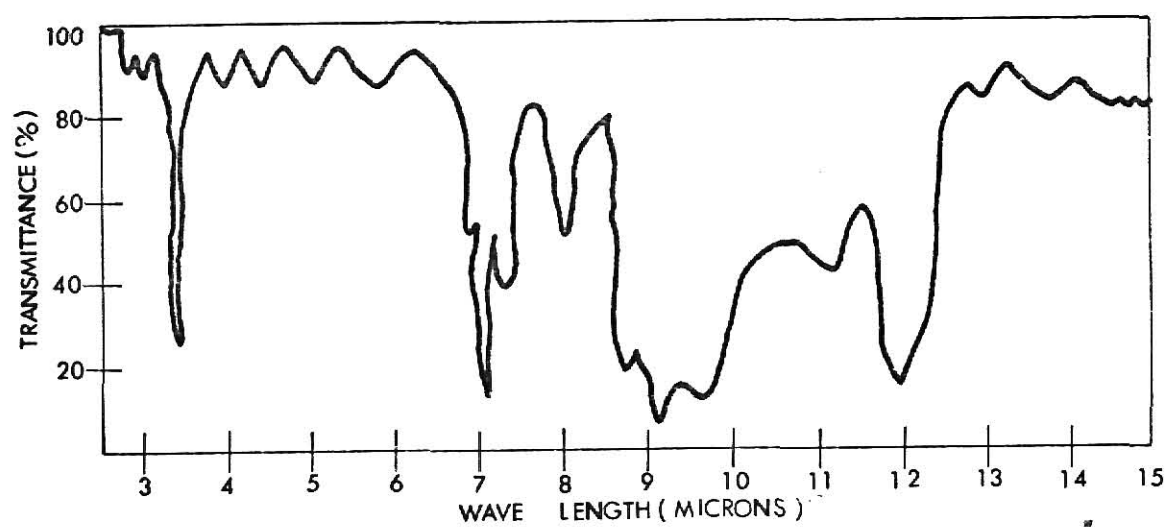


Figure 2. Transmittance of Tedlar at Long Wave Length Spectrum

Tedlar is a fully acceptable substitute for glass as the cover of flat plate solar collectors during day time.

At night, the transmissivity of Tedlar at thermal radiation is higher than that of glass such that Tedlar covered collector can lose a lot of heat from the collector plate by nocturnal sky radiation. The transmittance-wavelength curve for Tedlar is shown in Figure 1 and Figure 2 (22). For the purpose of engineering calculation, the transmittance of Tedlar for long-wave radiation was recommended as 0.3, and the emissivity of Tedlar was recommended as 0.63 (23).

Tedlar is resistant to oxidation, hydrolysis, depolymerization, and other degradation reactions (24). This inertness is especially noticeable in its resistance to weathering. Kalb (25) exposed Tedlar to the south at an angle of  $45^{\circ}$  to the horizontal in Florida for 16 years and showed that it was still clean, tough, flexible, and inert.

Because of these special properties of Tedlar, Tedlar was selected as the cover material in this study.

#### The Magnitude of Night Sky Radiation

Several techniques have been developed to calculate the net outgoing thermal radiation from a surface located on the earth. With aerological data, Picha and Villanueva (4) show that the radiation flux can be computed by use of Elsassen's chart and the technique developed by Simpson. In the absence of aerological data, Brunt (3) proposed the following universal equation for thermal radiation to a cloudless sky:

$$q_{cs} = \epsilon_p \sigma T_p^4 [1 - (0.44 + 0.080\sqrt{e})] \quad (1)$$

where  $e$  is the partial pressure of water vapor in the atmosphere in millibars. This equation is based on experimental observations for thermal radiation

emitted to the night sky at locations throughout Europe. Brunt also includes the effect of cloud coverage:

$$q_{r,p-s} = q_{cs} (1 - 0.09N) \quad (2)$$

where  $N$  is the tenths of the sky covered by clouds. Picha and Villanueva (4) proposed an equation of the same form as Brunt's equation but with different constants:

$$q_{cs} = \epsilon_p \sigma T_p^4 [1 - (0.50 + 0.072\sqrt{e})] \quad (3)$$

for  $e$  in the range 16 through 30. This equation was based on experimental results of work in Atlanta, Georgia. Their expression for the effect of sky cover is:

$$q_{r,p-s} = q_{cs} (1 - 0.06N) \quad (4)$$

With a theoretical analysis, Bliss (2) derived an equation:

$$q_{cs} = \epsilon_{ap} \sigma T_a^4 \quad (5)$$

where  $\epsilon_{ap}$  is apparent emissivity as shown in Fig 3. He made a chart shown in Fig 4, which he recommended for use in most engineering problems requiring an estimate of the intensity of the atmospheric radiation upon a horizontal surface near ground level for clear days. From the Bliss Equation, Swinback (5) related the effective sky temperature to the local air temperature in the simple relationship:

$$T_s = 0.0552 T_a^{1.5} \quad (6)$$

Niles, Haggard, and Hay (13) also obtained an expression from the Bliss equation, for estimating the effective sky temperature:

$$T_s = (0.0037 T_{dp} - 0.208)^{0.25} T_a \quad (7)$$

where  $T_{dp}$  is the ground level dewpoint temperature. If the effective sky temperature is known, the net thermal radiation exchange between a surface of

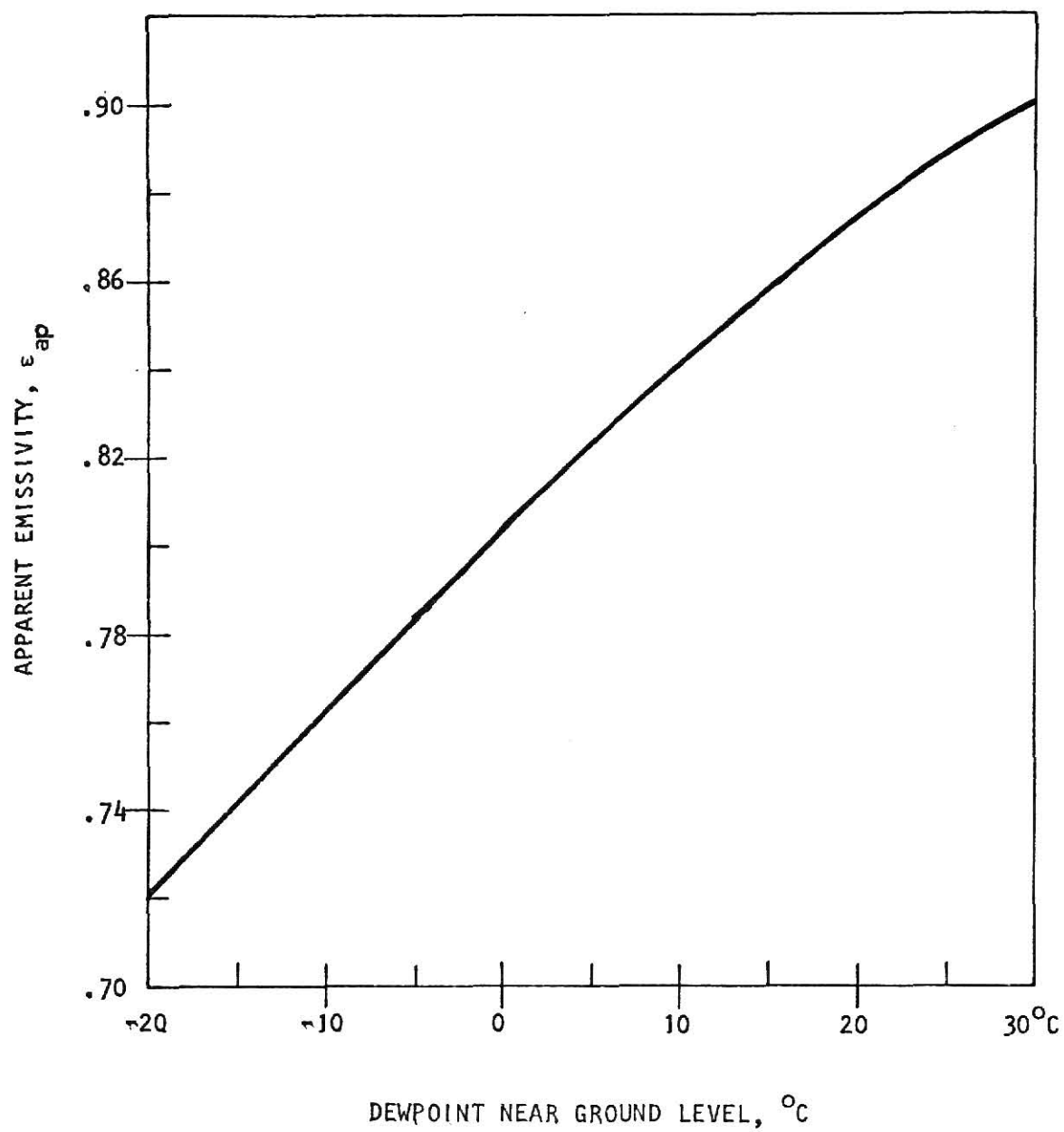


Figure 3. Typical Apparent Emissivity  $\epsilon_{ap}$  of a Clear Sky at Sea Level



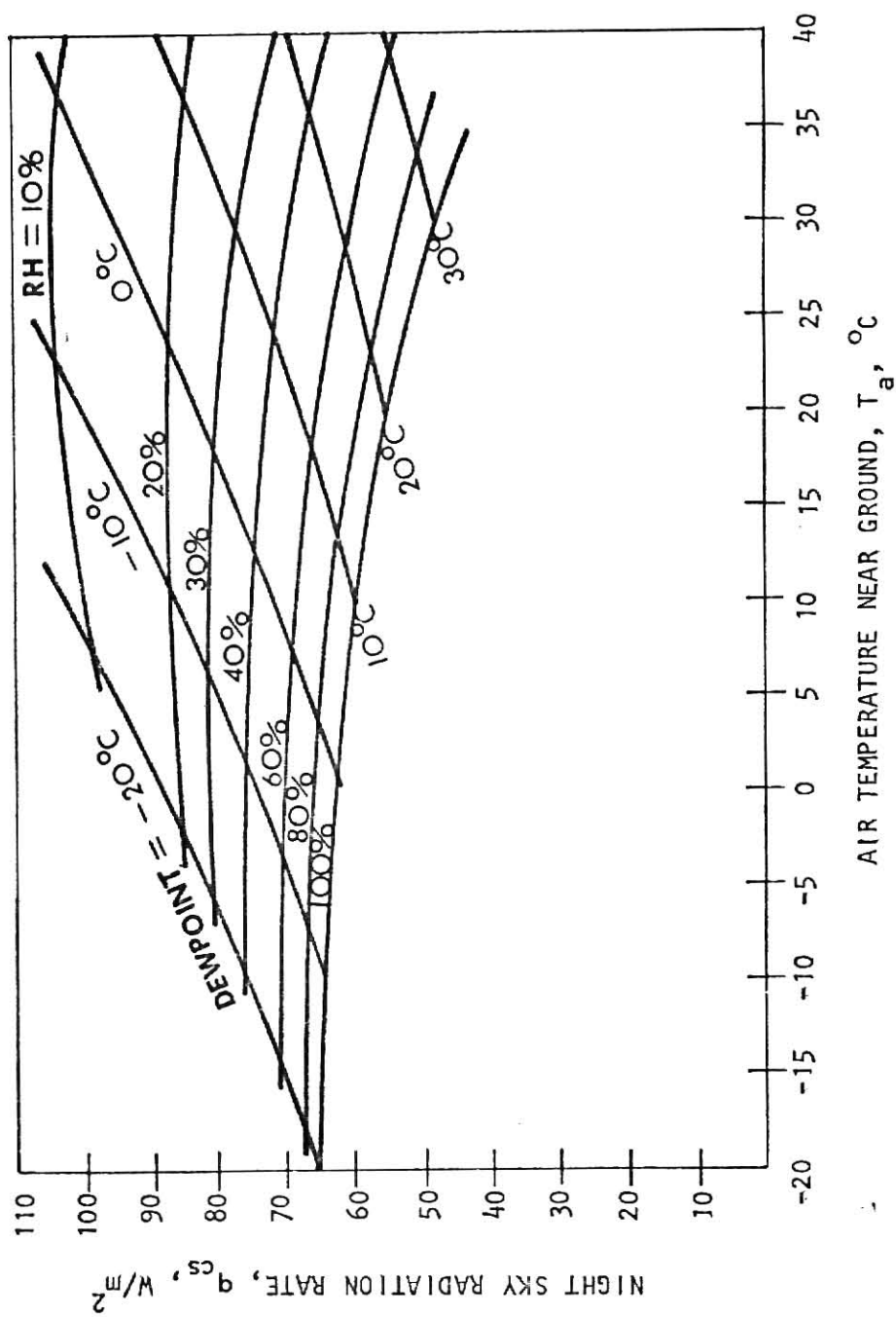


Figure 4. Typical Values of Night Sky Radiation for Clear Skies at Sea Level)

emissivity  $\epsilon_p$  and temperature  $T_p$ , and the sky radiation may be computed by:

$$q_{cs} = \epsilon_p \sigma (T_p^4 - T_s^4) \quad (8)$$

If the effect of cloud coverage is considered, equation (2) or equation (4) would have to be used with equation (8).

#### Practical Use of Night Sky Radiation

Nocturnal Sky Radiation has been used by man for cooling purposes for thousands of years. Archaeological evidence exists that "Ice Walls" were built in the Middle East. These, known as Yakh-chals, were mud walls running east-west, with basins on the north side in which water was frozen by nocturnal radiation. There are many examples of ice being made by night-sky radiation in olden times (26). In recent years, Thomason (10,11) reports some success in cooling during nights by allowing water from his 1,600 gallon storage tank to run down the unglazed north slope of his roof. An experimental heating-cooling system in southern Arizona (12) used a bare, water-circulating solar heat collector to collect heat in the winter, and to reject heat by night sky radiation in the summer. The heated or cooled water was stored in an insulated tank and circulated through ceiling panels in the building to provide necessary heating or cooling. An auxiliary conventional heat pump was used to further raise or lower the water temperature when necessary.

The recently constructed house at Phoenix, Arizona (16) which used a movable insulated roof in thermal contact with a metallic ceiling to absorb and retain solar heat in winter and to dissipate summer heat gain to the night sky, was proved to maintain room temperature between 68°F and 82°F through a normal year of Phoenix weather without supplementary heating or cooling, although the ambient temperature range was from subfreezing to 115°F.

## CHAPTER III

### THE MODEL

The purpose of this investigation was to compare the nocturnal radiation performance of two different kinds of radiators, namely, a radiator without cover and a radiator with cover, at the same night sky radiation. The analysis presented here follows the basic derivation idea for the solar flat plate collector by Duffie and Beckman (27), Whillier (23), and Hotel (28).

#### General Considerations

The performance of a water heated nocturnal radiator is described by an energy balance: the total energy loss from the radiator is equal to that of the water. The steady state energy balance on the whole radiator, as shown in Figure 5, can be written as

$$Q_{w-p} = Q_{r,p-s} + Q_l \quad (9)$$

where  $Q_{w-p}$  = rate of energy transferred from the water to the plate;

$Q_{r,p-s}$  = rate of energy loss by nocturnal sky radiation;

$Q_l$  = rate of energy loss from the radiator to the surroundings by convection, by radiation, and by conduction through supports.

The rate of energy loss by nocturnal sky radiation,  $Q_{r,p-s}$ , was discussed in the previous chapter. Equation (1), (3), (5), and (8) can be used to compute the magnitude of nocturnal sky radiation heat loss on a clear day. The values of nocturnal radiation obtained from these equations are very similar to one another. Among them Equation (8) is considered because of its simplicity to obtain the value of nocturnal sky radiation with less data. To use Equation (8),

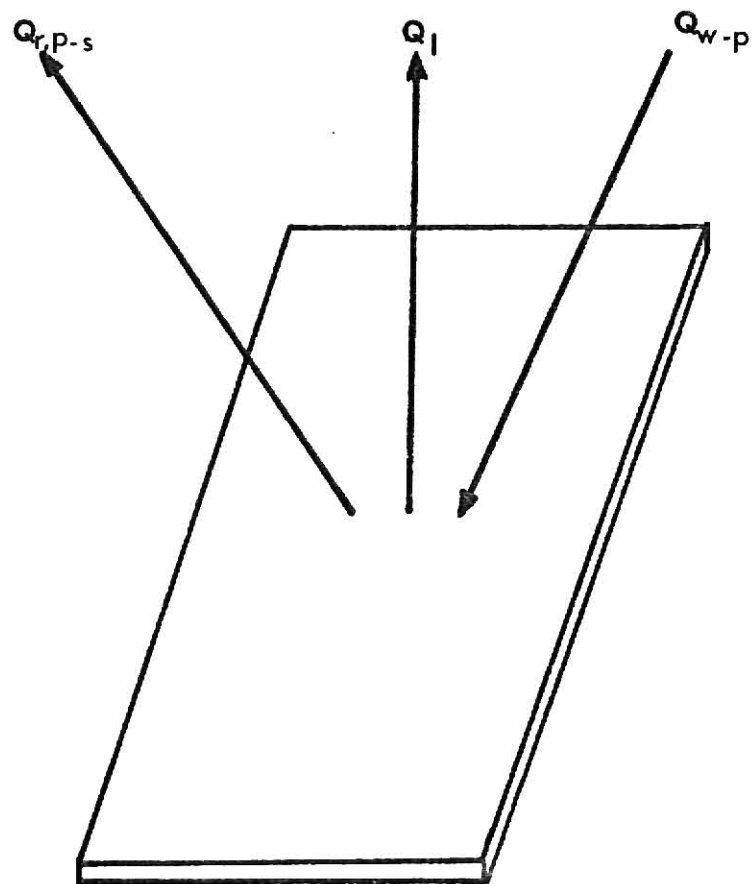


Figure 5. Energy Balance on the Plate

the value of effective sky temperature is needed. Equation (6) is used instead of equation (7) because of its simplicity. Equation (2) and Equation (4) represent the effect of cloud coverage for the night sky radiation. Equation (2) is the experimental results in Europe. On the contrary, equation (4) is the experimental results in U.S. So equation (4) is used for the effect of cloud coverage. From equation (4) and (8), the following equation is considered in this analysis

$$q_{r,p-s} = \epsilon_p \sigma (T_p^4 - T_s^4) (1 - 0.06N) \quad (10)$$

where the value of  $T_s$  can be found from equation (6).

To model the radiator, a number of simplifying assumptions are made without obscuring the basic physical situation. These important assumptions are:

1. Performance is steady-state.
2. There is one-dimensional heat flow to the atmosphere.
3. There is one-dimensional heat flow through back-insulation.
4. The sky is considered as a blackbody for long-wavelength radiation at an equivalent sky temperature.
5. Properties are independent of temperature.
6. Loss through front and back are to the same ambient temperature  
(This assumption is discussed later.)
7. Dust and dirt on the radiator are negligible.
8. The surroundings of the radiator is clear.

For the radiator with cover, the following assumptions are added:

9. There is no net energy absorption by the cover.
10. There is one-dimensional heat flow through the cover.
11. The temperature drop through cover is negligible.

### Radiator without Cover

Based on the above assumptions, the thermal network for bare flat-plate radiator is shown in Figure 6. The concept of an overall loss coefficient is used in order to simplify the mathematics. At some typical location on the plate where the temperature is  $T_p$ , the energy rejection from the plate is absorbed from the water,  $Q_{w-p}$ . The plate rejects its heat by nocturnal sky radiation,  $Q_{r,p-s}$ , which was stated a previous section, and by losses through the top and bottom of the radiator.

The energy loss through the bottom of the radiator is represented by  $R_1$ ,  $R_{2,c}$  and  $R_{2,r}$ .  $R_1$  represents the resistance to heat flow through the insulation and  $R_{2,c}$  and  $R_{2,r}$  represent the convection and the radiation resistance to the environment. The magnitude of  $R_{2,c}$  and  $R_{2,r}$  is usually so small that it is possible to assume  $R_{2,c}$  and  $R_{2,r}$  are zero and all resistance to heat flow is due to the insulation. Thus, the bottom loss coefficient,  $U_b$ , is

$$U_b = \frac{1}{R_1} = \frac{k}{L} \quad (11)$$

where  $k$  and  $L$  are the insulation thermal conductivity and thickness, respectively.

The resistance,  $R_3$ , from the plate to the surroundings through top depends on the speed of the wind blowing over the collector. McAdams (29) and others (27,6), relate the heat transfer coefficient to the wind velocity. The heat transfer coefficient from a flat plate exposed to outside winds is

$$h_{wind} = 5.7 + 3.8V \quad (12)$$

where  $V$  is the wind velocity, meter/second. Therefore, the top loss coefficient  $U_t$  is,

$$U_t = h_{wind} = 5.7 + 3.8V \quad (13)$$

From assumption 6., the bottom loss coefficient,  $U_b$ , has the same base temperatures as the top loss coefficient. So, the loss coefficient,  $U_1$ , shown in Figure 7, can be expressed as

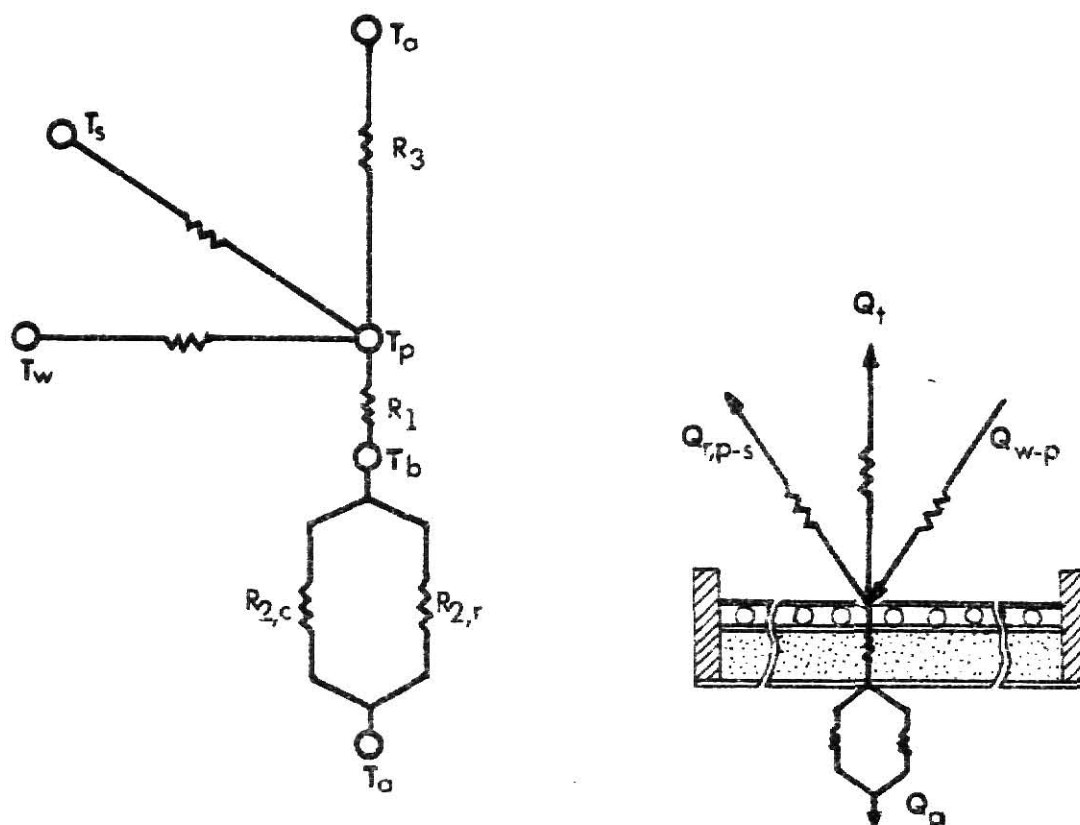


Figure 6. Thermal Network for Bare Flat-Plate Radiator

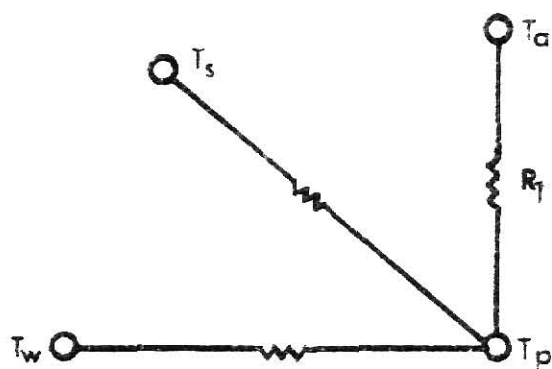


Figure 7. Equivalent Thermal Network for Bare Flat-Plate Radiator

$$U_l = U_t + U_b \quad (14)$$

Therefore, the rate of energy loss from the radiator to the surroundings by convection, and by conduction through supports is

$$Q_l = A_p U_l (T_p - T_a) \quad (15)$$

where  $A_p$  is the area of the radiator.

The rate of energy loss from the water,  $Q_{w-p}$ , is found from the water temperature difference. This value is

$$Q_{w-p} = \dot{m}C(T_{w,i} - T_{w,o}) \quad (16)$$

where  $\dot{m}$  is mass flow rate,

$T_{w,i}$  and  $T_{w,o}$  are inlet water temperature and outlet water temperature, respectively.

From the above equations, outlet water temperature of the bare collector,  $T_{w,o}$ , is

$$T_{w,o} = T_{w,i} - \frac{A_p \left[ (5.7 + 3.8V + T) \left( T_p - T_a \right) + \epsilon_p \sigma (T_p^4 - T_s^4) (1 - 0.06N) \right]}{\dot{m}C} \quad (17)$$

#### Radiator with Cover

The main differences between the uncovered radiator and the covered radiator are the loss coefficient for the top surface and the value of loss for nocturnal sky radiation. As shown in Figure 8,  $R_{3,c}$  and  $R_{3,r}$  are the result of natural convection and radiation between plate and cover.  $R_{4,c}$  is the convection heat resistance between the cover and the atmosphere, depending on wind speed.  $R_{4,r}$  is the radiation resistance from the cover to the sky.

For the natural convection resistance,  $R_{3,c}$ , Tabor (30) has examined the published results of many investigations and concluded the most reliable data for use in solar collector calculations. He recommends the following relationships for air between horizontal planes:



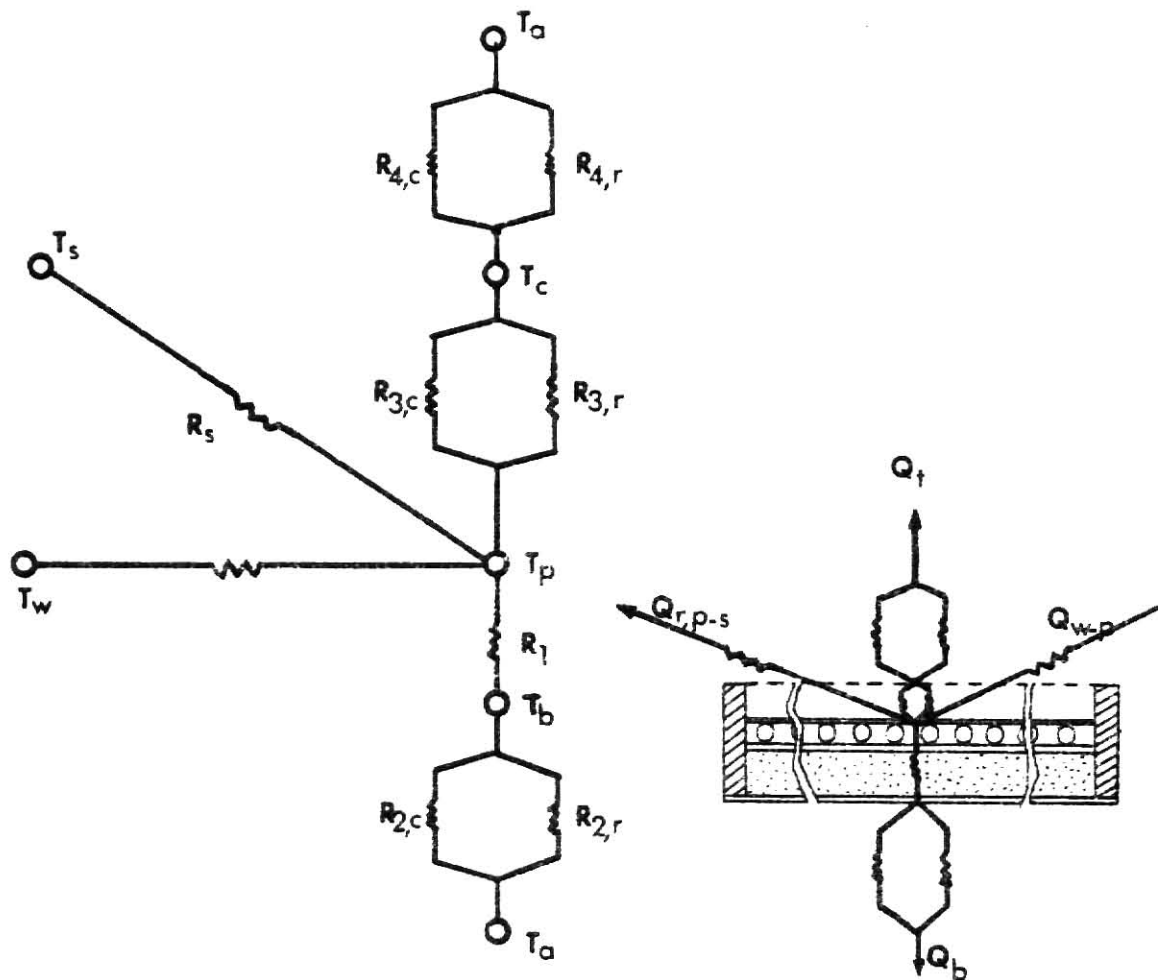


Figure 8. Thermal Network for Covered Flat-plate Radiator

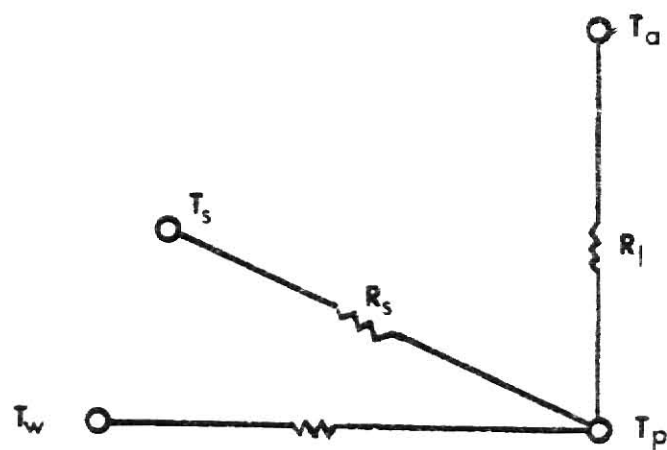


Figure 9. Equivalent Thermal Network for Covered Flat-plate Radiator.

$$Nu = 0.152 (Gr)^{0.281} \quad (18)$$

where  $10^4 < Gr < 10^7$ . Duffie and Beckman (27) rewrote Equation (18) in dimensional form:

$$h_{10} = 1.613 \frac{\Delta T^{0.281}}{l^{0.157}} \quad (19)$$

where  $h$  is in  $W/m^2 \text{ } ^\circ C$ ,  $\Delta T$  is in degree Celsius,  $l$  is the plate spacing in centimeters, and air properties are evaluated at the average of plate and cover temperatures taken here as  $10^\circ C$ . For air temperature other than  $10^\circ C$  they used the following equation to correct for temperature variations:

$$\frac{h_{3,c}}{h_{10}} = 1 - 0.0018 (\bar{T} - 10) \quad (20)$$

where  $\bar{T}$  is the average temperature between plate and cover. Whillier (23) also proposed a very simple relationship for the natural convection coefficient:

$$h_{3,c} = 1.5774 (T_p - T_c)^{0.25} \quad (21)$$

The results from equation (21) are almost the same as those from equation (20). For simplicity equation (21) was selected in this study. When the temperature of the cover is greater than that of the plate the natural convection loss is zero.

Radiation heat loss between plate and cover can be expressed as (31)

$$\frac{Q_{r,p-c}}{A_p} = \frac{\sigma(T_p^4 - T_c^4)}{1/\epsilon_p + 1/\epsilon_c - 1} \quad (22)$$

If the radiation term is linearized to the temperature difference between plate and cover, the radiation heat transfer coefficient is

$$h_{3,r} = \frac{\sigma(T_p + T_c)(T_p^2 + T_c^2)}{1/\epsilon_p + 1/\epsilon_c - 1}$$

Therefore, total resistance between plate and cover,  $R_3$ , can be expressed as

$$R_3 = \frac{1}{h_{3,c} + h_{3,r}} \quad (24)$$

Equation (12) can be used to calculate the convection heat transfer coefficient between the cover and the air.

$$h_{4,c} = 5.7 + 3.8V \quad (25)$$

The radiation heat loss from the cover to the sky can be expressed as (31)

$$\frac{Q_{r,cs}}{A_c} = \epsilon_c \sigma (T_c^4 - T_s^4) \quad (26)$$

where  $\epsilon_c$  is the emissivity of the cover. For simplicity, if this radiation heat loss is linearized to the difference of temperature between cover and ambient, the radiation conductance can be written as

$$h_{4,r} = \frac{\epsilon_c \sigma (T_c^4 - T_s^4)}{(T_c - T_a)} \quad (27)$$

where  $T_a$  is the ambient temperature. The resistance from the cover to the surroundings is then given by

$$R_4 = \frac{1}{h_{4,c} + h_{4,r}} \quad (28)$$

Thus, for the covered radiator the top loss coefficient from the plate to the ambient may be written

$$U_t = \left( \frac{1}{h_{3,c} + h_{3,r}} + \frac{1}{h_{4,c} + h_{4,r}} \right)^{-1} \quad (29)$$

It is difficult to determine the cover temperature. Duffie and Beckman (32) recommend an iteration method to find the cover temperature. The heat loss from the plate to the cover is the same as that from the plate to the surroundings, assuming no storage in the cover. The heat balance on the cover can then be rearranged to read the cover temperature:

$$T_c = T_p - \frac{U_t (T_p - T_a)}{h_{3,c} + h_{3,r}} \quad (30)$$

The iteration method is to assume first the cover temperature between the temperature of plate and that of ambient, but nearer ambient temperature, and

then calculate the top loss coefficient from Equation (29). By using Equation (30), it is possible to calculate the cover temperature and compare this value with the assumed cover temperature.

The top loss coefficient can be combined with the bottom loss coefficient because of its same base temperature. The loss coefficient,  $U_1$ , shown in Figure 9, can be expressed as in Equation (14). Equation (15) also can be used for the covered collector.

The cover is partially transparent to thermal radiation. Because of that, the nocturnal sky radiant heat transfer of the covered collector from plate to sky should have to be modified. From equation (10), the nocturnal sky radiant component is

$$q_{r,p-s} = \zeta \epsilon_p \sigma (T_p^4 - T_s^4) (1 - 0.6N) \quad (31)$$

where  $\zeta$  is the transmissivity of the cover material.

Combining all above equations, the outlet water temperature of the covered collector,  $T_{w,o}$ , can be written as following:

i)  $T_p > T_c$

$$T_{w,o} = T_{w,i} + \frac{\frac{A_p \zeta \epsilon_p \sigma (T_p^4 - T_s^4) (1 - 0.6N)}{\dot{m}C} - \frac{A_p (T_p - T_a)}{\dot{m}C}}{\left( \frac{1}{1.5774(T_p - T_c)^{0.25} + \frac{\sigma(T_p + T_c)(T_p^2 + T_c^2)}{(1/\epsilon_p + 1/\epsilon_c - 1)}} + \frac{1}{5.7 + 3.8V + \frac{\epsilon_c \sigma (T_c^4 - T_s^4)}{T_c - T_a}} \right)^{-1}} \quad (32)$$

ii)  $T_p \leq T_c$

$$T_{w,o} = T_{w,i} + \frac{\frac{A_p \zeta \epsilon_p \sigma (T_p^4 - T_s^4) (1 - 0.6N)}{\dot{m}C} - \frac{A_p (T_p - T_a)}{\dot{m}C}}{\left( \frac{1/\epsilon_p + 1/\epsilon_c - 1}{\sigma(T_p + T_c)(T_p^2 + T_c^2)} + \frac{1}{5.7 + 3.8V + \frac{\epsilon_c \sigma (T_c^4 - T_s^4)}{T_c - T_a}} \right)^{-1}} \quad (33)$$

Usually, the edge loss in the radiator is very small so that it is not necessary to consider this loss. Tabor (30) recommends that the edge losses can be estimated by assuming one-dimensional sideways heat flow around the perimeter of the radiator. His equation for the edge loss rate is

$$Q_e = A_e C_e \quad (34)$$

where  $A_e$  is the area of edge and  $C_e$  is conductance of side material.

## CHAPTER IV

### EXPERIMENTAL WORK

The goal of this investigation was to compare the temperature drop between a Tedlar-covered collector and an uncovered collector at different flow rates and different input temperatures.

#### General Description of Test Facility

Four collectors were used for this study. Figure 10 shows the schematic view of the test facility. The entire assembly was installed on the roof of the west wing of Seaton Hall at Kansas State University in Manhattan, Kansas.

Main components of the system were:

1. Two collectors without cover.
2. Two collectors with Tedlar as cover.

The auxiliary components of the system were:

1. A constant temperature circulator.
2. Two valves to vary the flow rate.

The instrumentation was:

1. Water flow meters.
2. Copper-constantan thermocouples to measure plate and water temperature.
3. A multipoint potentiometer to measure the e.m.f. of thermocouples.
4. Mercury thermometers to measure the wet-bulb and dry-bulb temperature.

#### Test Collectors

Four similar test collectors, two with Tedlar as the cover and two without covers, were designed and constructed for this investigation. The four collec-

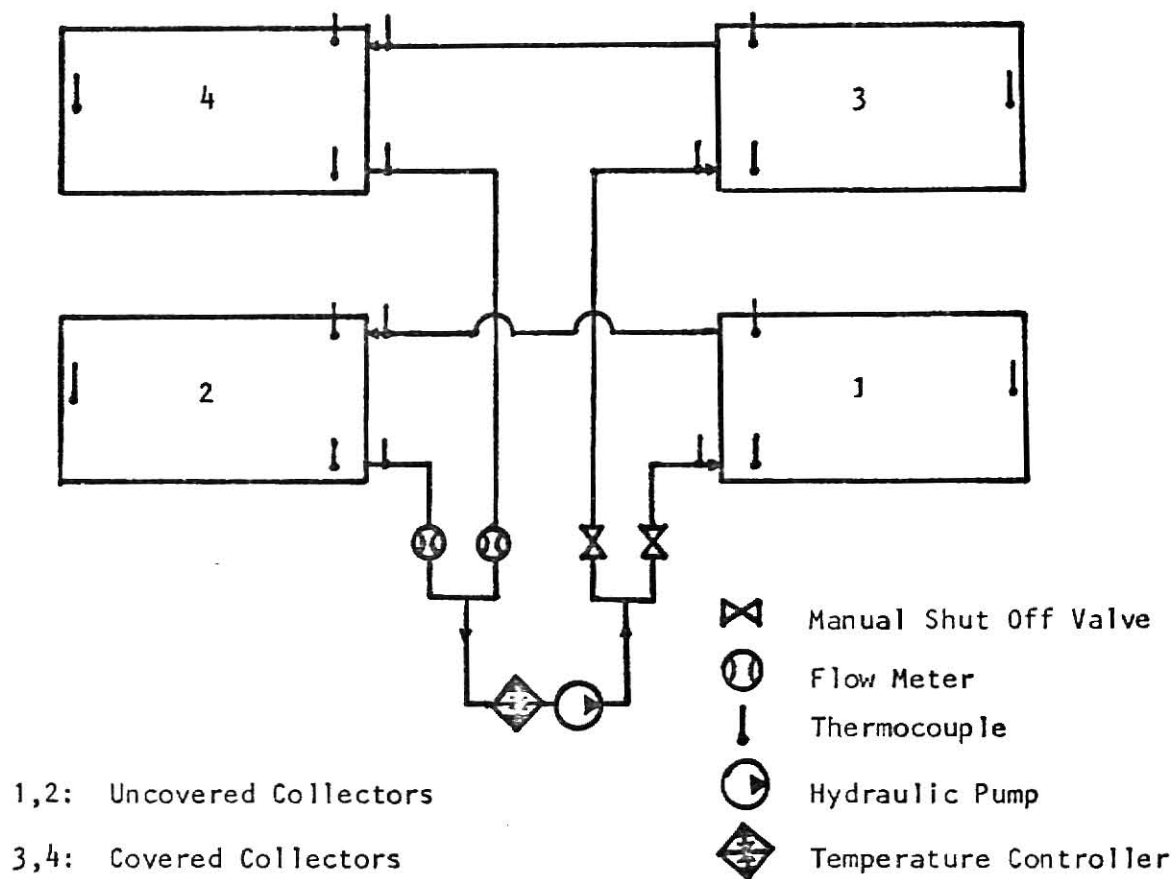


Figure 10. Schematic Diagram of the Test Apparatus

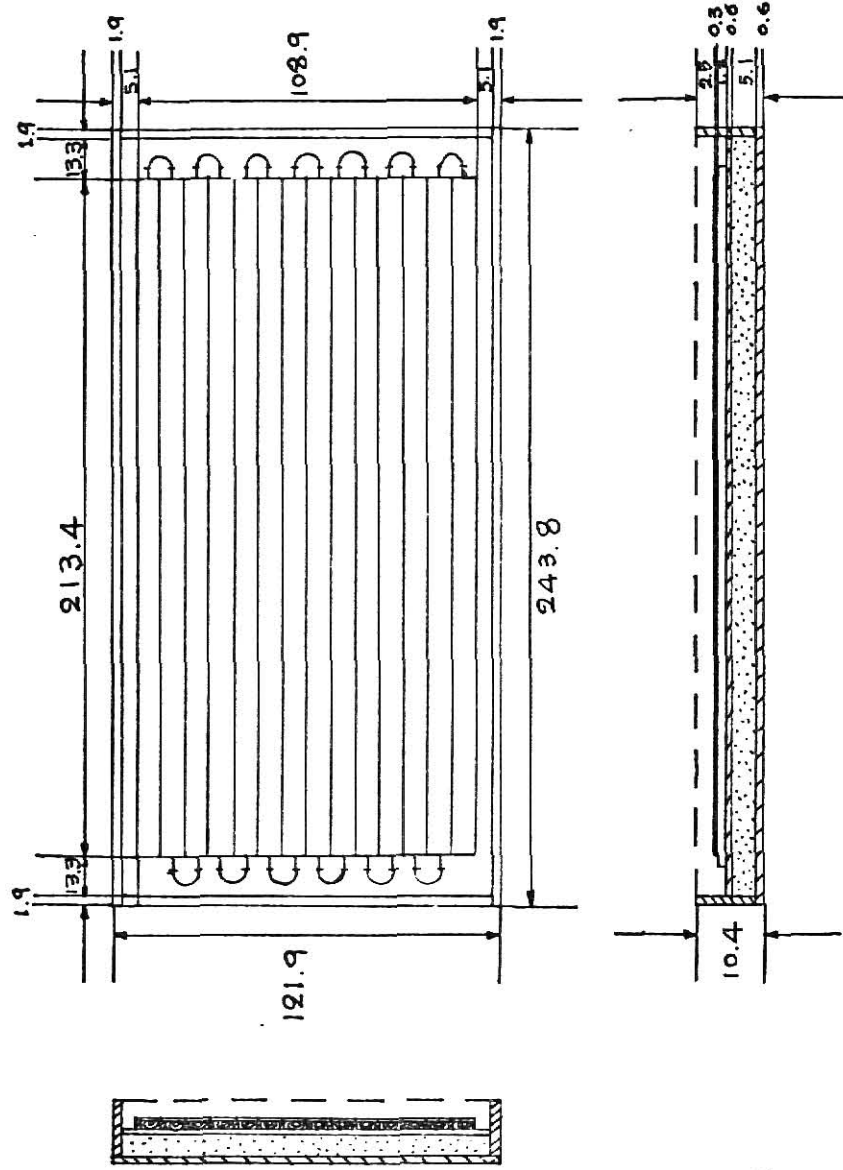


Figure 11. A Schematic Diagram for Collector



tors were mounted horizontally on the roof. The two collectors of each kind were connected so that the water flowed through them in series. Thus each kind of collector consisted of two identical sections. The reason for using two sections was to provide a larger surface area and thus a larger water temperature drop than could be obtained with a single section. Assuming the same absolute accuracy of temperature measurement, the larger temperature drop would yield a smaller percentage error. An auxiliary benefit was the ease of water temperature determination "half way" through each collector. Figure 11 shows a schematic diagram of the collectors. The only significant difference between collectors is that those with the covers had Tedlar sheets 2.5cm above the plates. The same construction was used for all collectors, details of which are shown in Figure 12. Expanded polystyrene extruded foam insulation, 118.1cm by 240cm by 5.1cm thick, which was used as an insulation material. This insulation was put in the bottom of a box that was made from a piece of plywood as the bottom of box, 121.9cm by 243.8cm by 0.6cm thick, two pieces of wood as short length sides of box, 7.3cm by 118.1cm by 1.9cm thick, and two pieces of wood as long length sides of box, 7.3cm by 243.8cm by 1.9cm thick. On the top of this foam insulation a piece of plywood, 118.1cm by 240cm by 0.6cm thick, was used as a base for the emitter plate.

The emitter plate was made up of aluminium plate and tube, integrally extruded, with dimensions of 7.6cm by 0.3cm for the strip and 1.3cm for the tube outside diameter. Fourteen pieces, each 213.4cm long were placed side-by-side thus yielding a total plate surface area of  $2.27 \text{ m}^2$ . The tubes were interconnected with rubber hoses and clamps. The top surface of the plates were painted flat black paint having an emissivity of approximately 0.96 (23). On the two collectors having covers, a wood frame served to hold the Tedlar sheets a distance of 2.5cm above the plates.

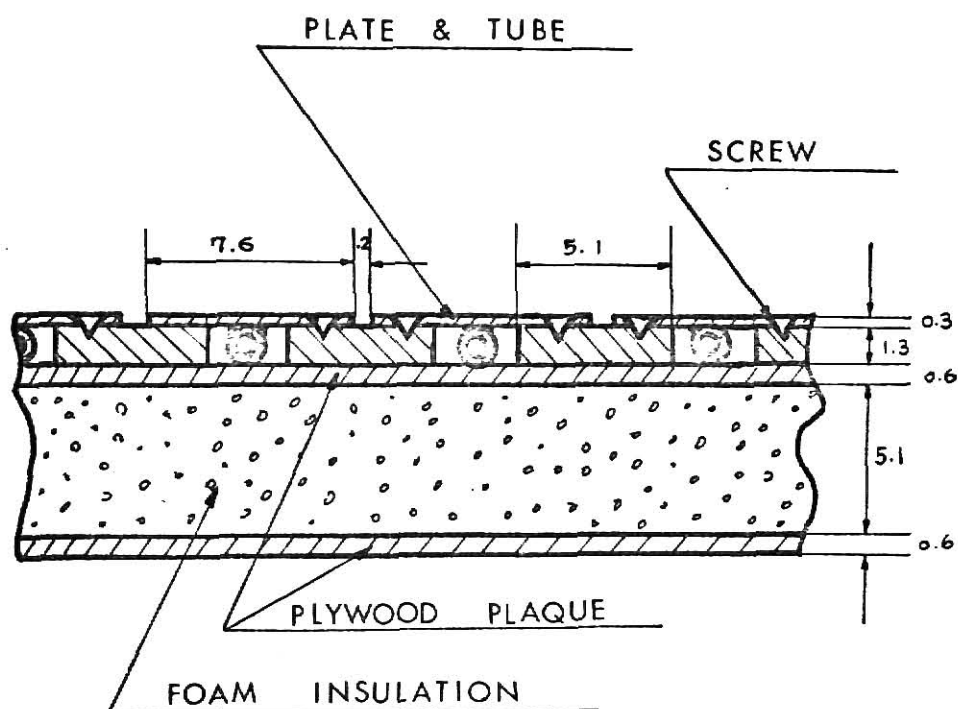


Figure 12. Construction Details of the Collector

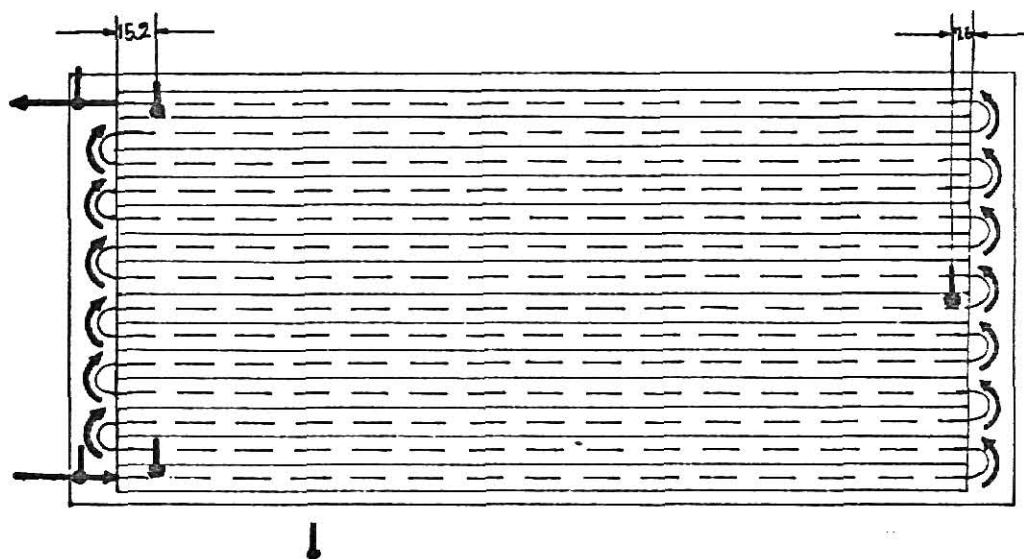


Figure 13. Flow Pattern Through Radiator and Location of Thermocouples

### Water Supply System

Water was supplied by the pump, which had a capacity of 10 liters/min, in a Constant Temperature Circulator, Model FT made by Polyscience Corporation. As shown Figure 10, water flowed into the two different kinds of collectors simultaneously, at the same inlet temperature and at the same flow rate, then returned back to the Constant Temperature Circulator. The water inlet temperature was controlled by setting the temperature adjusting knob on the Constant Temperature Circulator. The control temperature range of it was  $-60^{\circ}\text{C}$  to  $250^{\circ}\text{C}$  with an accuracy  $\pm 1.0^{\circ}\text{C}$ . The heater input was 1000 watts maximum.

The flow rate was varied by adjusting the openings of two shut-off valves which were located after the pump. The flow pattern through each collector was as shown in Figure 13.

### Instrumentation

All the temperatures were measured by copper-constantan thermocouples of 24 B&S gage wire. Before installing, all thermocouples were calibrated against the melting ice temperature. Their e.m.f. output was measured by a Honeywell Eroctronik 16, multi strip chart recorder.

Thermocouples were mounted inside of the pipe at the inlet and outlet of each collector to measure the water temperature. Three thermocouples per one collector were used to establish the mean plate temperature. These thermocouples were attached to the underside of the aluminium plate at various positions. One thermocouple, hung in the air, read the atmospheric temperature. The exact positions are shown in Figure 13.

Variable area orifice meters were used to measure the water flow rate. They were calibrated by stopwatch and scales before being connected to the test equipment. A linear least square regression model was used to obtain the

calibration curve. The flow rate was controlled by opening or closing two shut-off valves.

In order to find the partial pressure value of water vapor in the atmosphere, the wet-bulb and the dry-bulb temperatures were measured with a sling psychrometer.

For determining the tenths of cloud coverage, there is no generally accepted criterion at present (4). Not only is the cloud position important but also the height and physical composition are needed to decide the tenths of cloud more accurately (33). In the present investigation, the tenths of cloud coverage was assumed by judging from direct observation.

Wind velocity was estimated from information obtained from the cable television weather information service.

#### Testing Procedure

The test started by turning on the pump switch in the Constant Temperature Circulator at 7:00 p.m. of each day. The water level inside the tank was checked to ensure that the electric heater and pump were completely immersed. After installing the chart for continuous, automatic roll in the recorder, the power switch was turned on in order to allow a warm-up period of two hours before any readings were recorded. Protective covers, which were used to shield the collectors from dust and rain, and to prevent absorption of solar energy during daytime, were removed from the collectors. The flow rate was adjusted by opening or closing the manual valve in order to maintain the same given flow rate to the two different kinds of collectors. Temperature was set at the desired value by dialing temperature setting knob in the Constant Temperature Circulator.

At 8:30 p.m. of each day, the thermocouple recorder chart switch was

turned on, and temperatures and flow rates were observed. After reaching stable conditions, the following measurements were taken, commencing at 9:00 p.m.:

1. Inlet and outlet water temperatures of each collector.
2. Plate temperatures of each collector at three different places.
3. Ambient temperature.

In addition to the above readings, the water flow rates, and the ambient wet and dry bulb temperatures were measured. The tenths of cloudy coverage was estimated. Velocity of wind was obtained from cable television. At 7:00 a.m. of the next day, the testing was ended and the protective covers were replaced on the collectors.

After recording all the necessary data during night, the collector plates were painted again and the Tedlar cover were cleaned. After rearrangement, the same procedures, described earlier, were followed on subsequent nights.

It should be pointed out that every effort was made in the present investigation to maintain a constant flow rate and the same flow rate to the two different kinds of collectors.

## CHAPTER V

### RESULTS AND DISCUSSION

#### Experimental Results

During this study fifteen sets of overnight temperature data were taken from 1 August 1977 to 31 August 1977. The range of operating conditions and the number of experimental runs for each overnight data set are summarized in Table 1. The water flow rate and the entering water temperature was controlled. The flow rates were controlled at 119 cc/min, 238 cc/min, and 357 cc/min. The Tedlar covered collector of this investigation could be used practically as a night sky radiator for cooling during summer when the flow rates were between 119 cc/min and 357 cc/min. Much attention was paid to maintain the constant flow rates and the same flow rates to the two different kinds of collector because the purpose of this investigation was to compare two different kinds of collectors. The inlet water temperatures were controlled by adjusting the temperature setting knob on the Constant Water Circulator. The inlet water temperatures could not always be maintained constant because the heater input was insufficient. But if the inlet water temperatures were maintained between 30°C and 40°C, these temperatures could be accepted as good practical inlet temperatures. Three rainy-day test runs were made to check how the radiators work in rain.

Temperature measurements were recorded for each minute interval between 9:00 p.m. and 7:00 a.m. However, not all of these data were used in the analysis. In general, only hourly temperature readings were used. These were: ambient

Table I. Operating Conditions

Water Flow Rate cc/min	Inlet Water Temperature °K	No. of Runs
119	310	3*
119	305	3*
238	310	2
238	305	2
357	310	3*
357	305	2

\* One is rainy day

temperature, three inlet and outlet water temperature at two uncovered collectors, six plate temperature at two uncovered collectors, three inlet and outlet water temperature at two Tedlar-covered collectors, and six plate temperature at two Tedlar-covered collectors. Four other components were measured. These were: tenths of cloud, wind velocity, dry and wet bulb temperature, and flow rate.

Figure 14, 15, 16, and 17 show plots of temperature versus time for selected runs from the 15 data sets. The inlet water temperatures for these selected runs were  $310^{\circ}\text{K}$ . As mentioned earlier, each kind of collector consisted of two sections with water temperature measurements at the inlet and outlet of each section. Figure 14 is the data set for 9:00 p.m. 29 August to 7:00 a.m. 30 August. That night was very cloudy but not windy. The flow rate was 119 cc/min. As can be seen in Figure 14, the outlet water temperature was below the ambient temperature at the exit of the first section for both kinds of collectors.

Figure 15 is the data set from 9:00 p.m. 11 August to 7:00 a.m. 12 August. That night was not cloudy and not windy. The flow rate was 238 cc/min. The first section of the bare collector was sufficient to cool the outlet water temperature below the ambient temperature but this was not true for the covered collector.

Figure 16 is the data set from 9:00 p.m. 28 August to 7:00 a.m. 29 August. That night was a little cloudy and windy. The flow rate was 357 cc/min. The first section of both kinds of collectors could not cool the outlet water temperature below the ambient temperature.

Figure 17 shows the temperatures measured during a rainy night. These were obtained between 9:00 p.m. 27 August and 7:00 a.m. 28 August. The rain started at about 12:30 a.m. The water temperature control was set at  $310^{\circ}\text{K}$  but that temperature could not be maintained because of lack in heater capacity



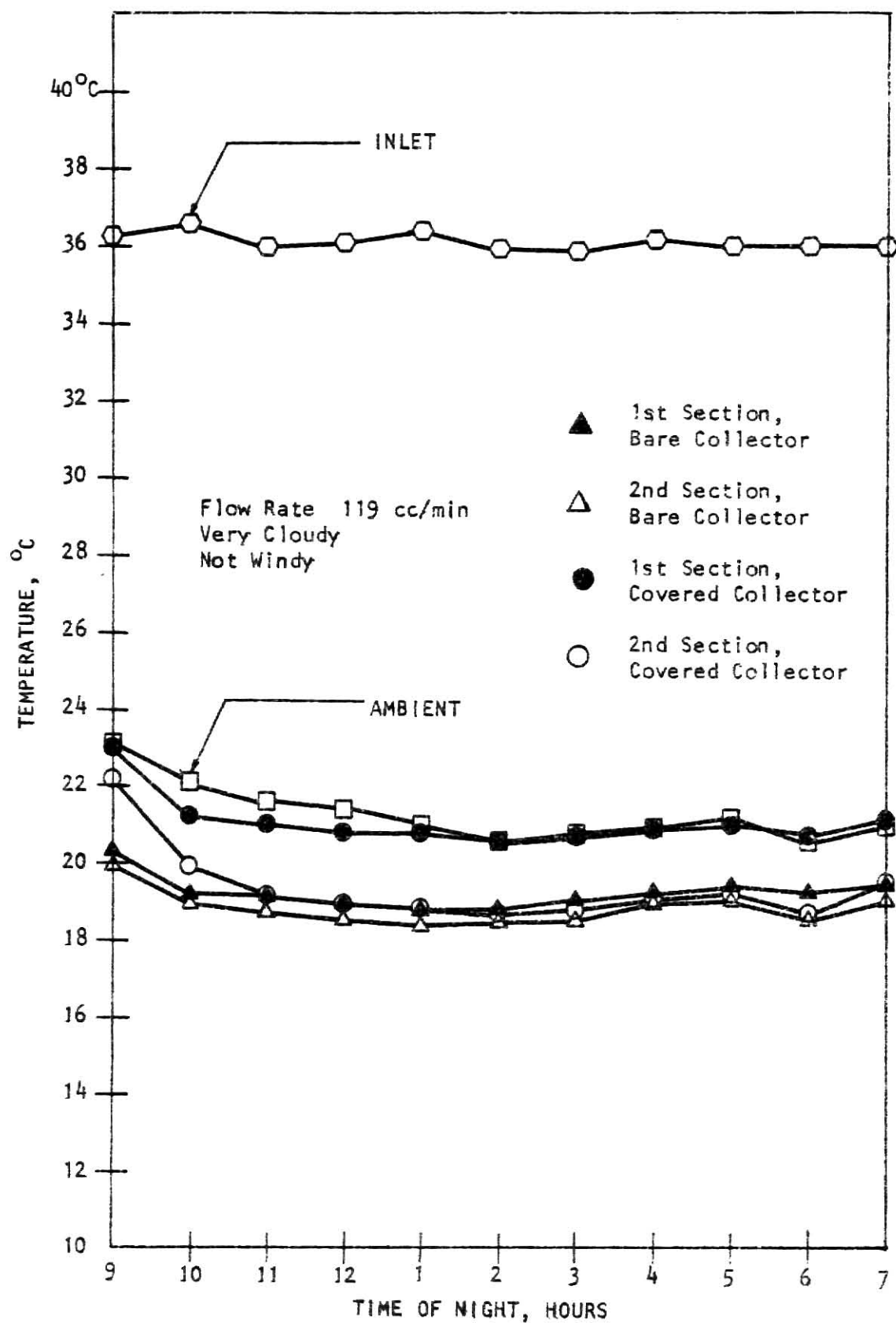


Figure 14. Actual Outlet Water Temperature at A Normal Night

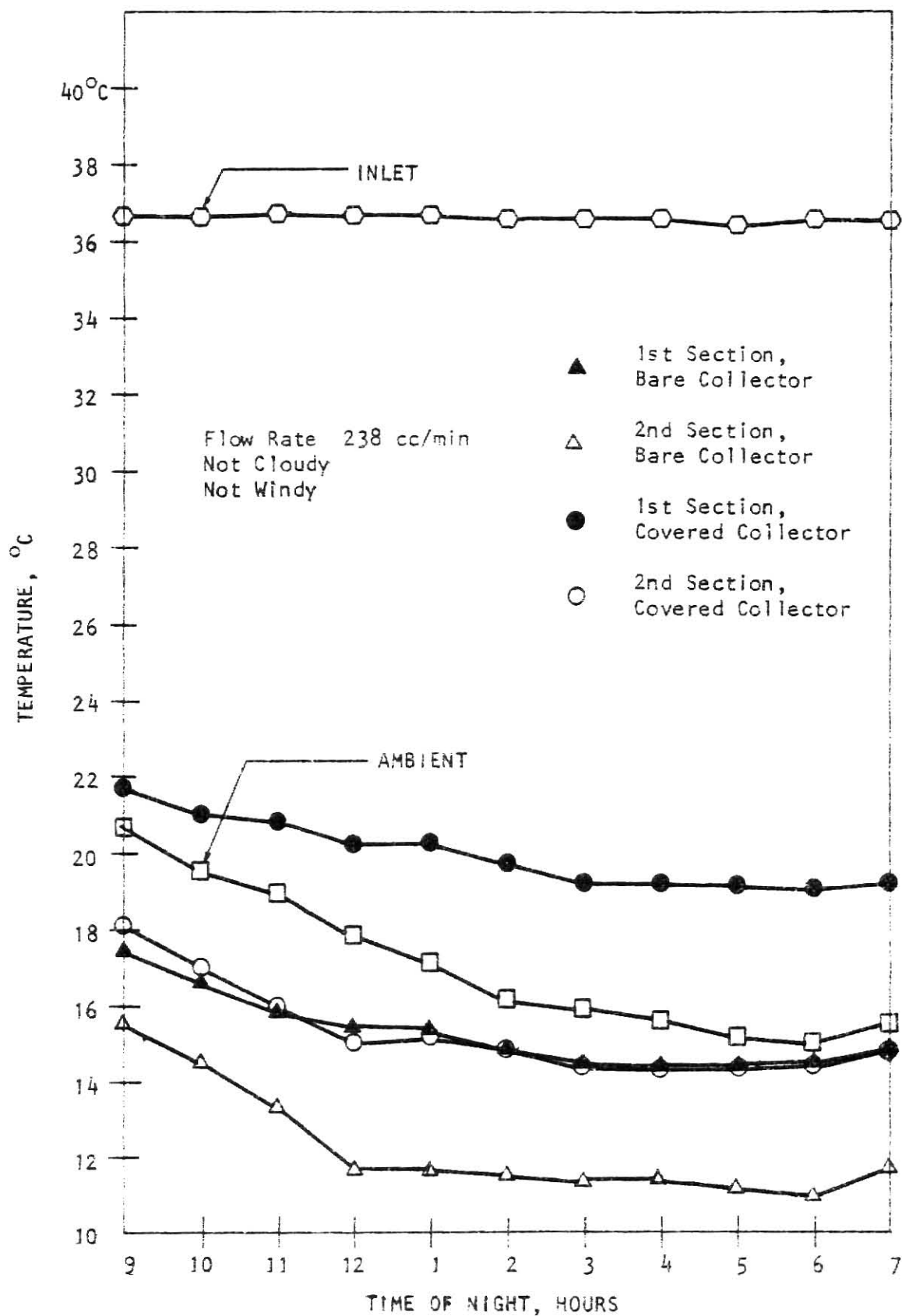


Figure 15. Actual Outlet Water Temperature at A Normal Night

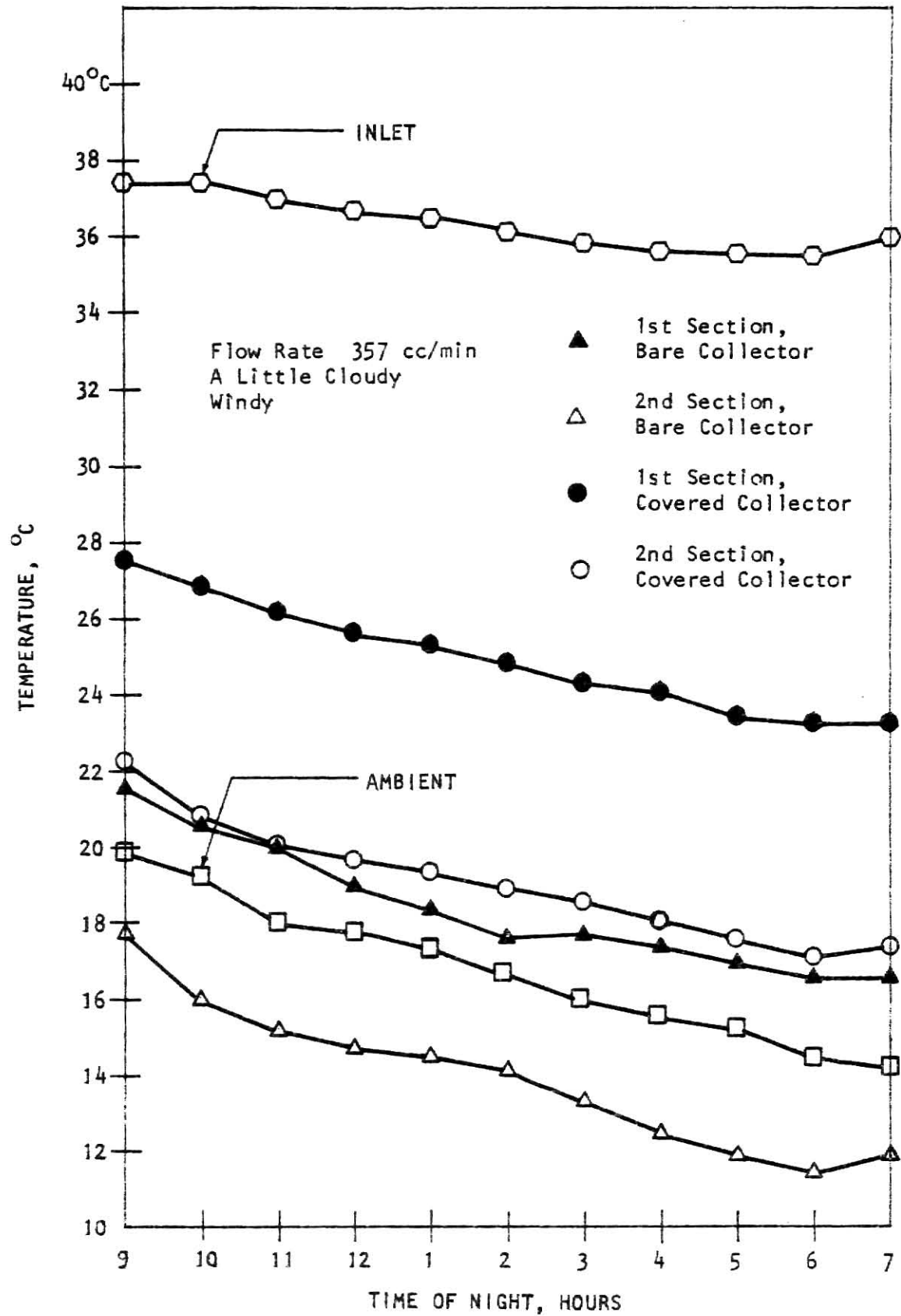


Figure 16. Actual Outlet Water Temperature at A Normal Night

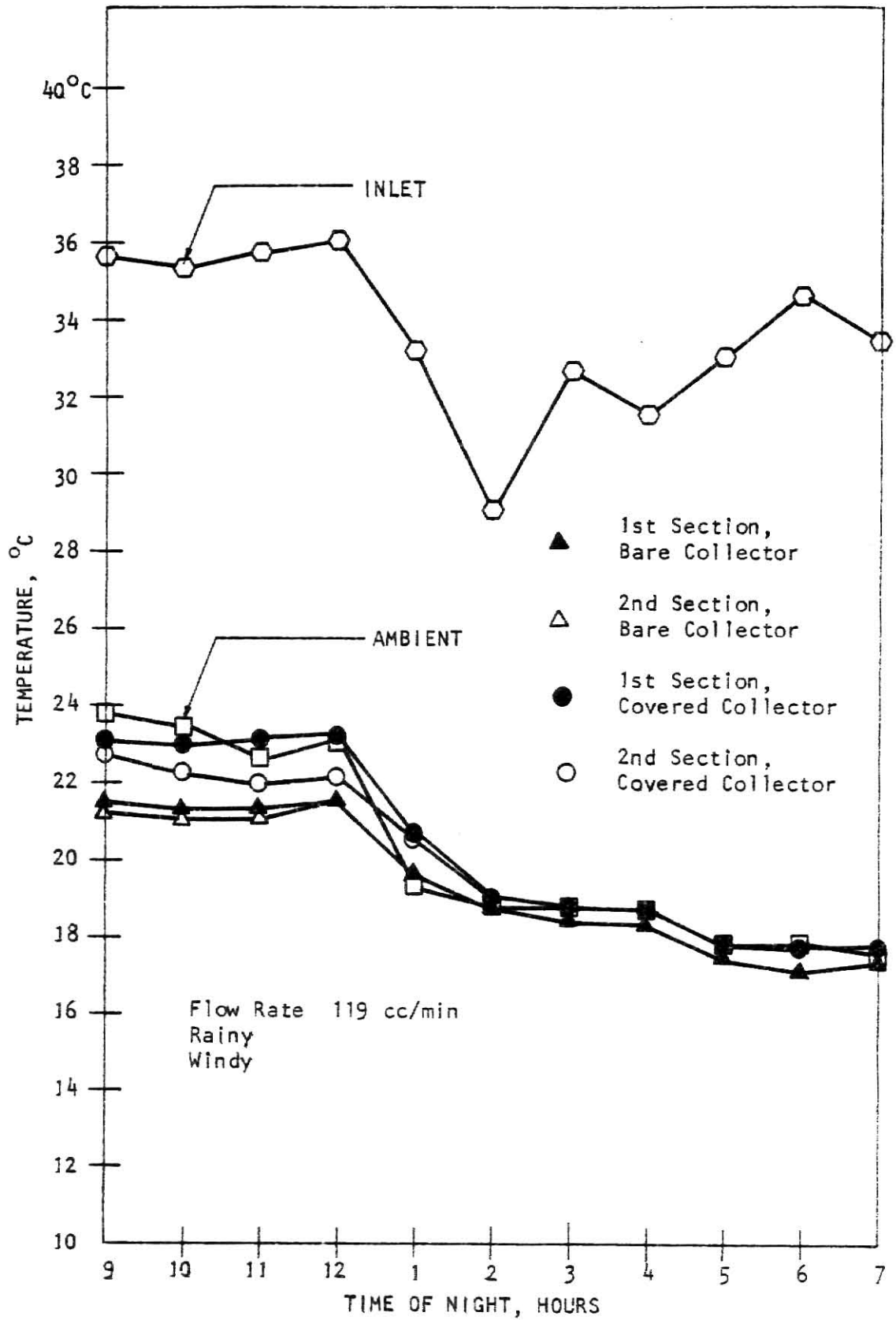


Figure 17. Actual Outlet Water Temperature at A Rainy Night

even though the flow rate was only 119 cc/min. During this night, the wind velocity was very high, 6 - 10 m/sec, and the rainfall was 6.5 cm. As can be seen in Figure 17, the outlet water temperatures were almost the same or a little lower than ambient temperature for both kinds of collectors.

The other eleven test runs yielded results similar to those shown. Based on all of the test results, the following observations can be made:

1. Even though the area of collectors was more than adequate, the outlet water temperature drop was limited for both kinds of collectors. The reason is that the value of nocturnal sky radiation loss finally will be same as that of heat gain from the surroundings. When the plate temperature was above the ambient temperature, the collector lost heat by convection, conduction as well as radiation. But if not, the collector gained heat by convection, conduction, and radiation from the surroundings equal in magnitude to the nocturnal sky radiation loss. This heat balance requirement fixed the minimum obtainable outlet water temperature.
2. The minimum outlet water temperature for both kinds of collector fully depended on the ambient temperature and weather conditions. It is generally observed that the limit of outlet water temperature drop was between  $2^{\circ}\text{C}$  and  $6^{\circ}\text{C}$  below ambient temperature, depending upon environmental conditions, for both kinds of collectors.
3. In rainy weather, the outlet water temperature of both kinds of collectors was the same or a little lower than ambient temperature unless the flow rate was very high.

### Comparison between Actual and Calculated Performance

A computer program was written by using the theory of the model section, Chapter III. The computer program for the model, listed Appendix B, was designed to calculate all of the heat loss quantities, the outlet water temperature, and the temperature difference between actual and calculated outlet water temperatures. Several values of constants and physical properties which were used for input to this program are listed in Table II. Those values were obtained from references (32, 23, 34) or calculated from the specifications of materials used. All other input data were obtained from the experimental results excepting the temperature of the cover. The cover temperatures were first assumed to be between the plate and the ambient temperature but nearer the ambient temperature and then computed using the iteration procedure described in Chapter III.

As mentioned earlier, exact values of tenths of cloud cover and of wind velocity were not obtained. So these values are known only to the extent of personal observation of the sky conditions as to cloud cover and cable television indications as to wind conditions. For the first test of the model, then a data set for a night with a clear sky and light winds was chosen.

Computations for each hour, on the hour, for the data between 9:00 p.m. 6 August and 7:00 a.m. 7 August are listed in Appendix C. At the beginning of Appendix C., all the variables of computer output are explained. FLOW, TEMPI, TEMPO, and TEMPP are measured data, and TEMPC, Q, QB, QEDGE, QRPS, QT, TEMPOC, and TEMPD are calculated values. That night when the data was obtained was very clear with variable light winds. Such night conditions are typical during the summer in Manhattan, Kansas. The entering water temperature of both kinds of collectors was  $306.2^{\circ}\text{K}$  and the flow rate was 357 cc/min. The values of wind velocity were observed to be between 1.79 m/sec and 3.57 m/sec. Because exact

TABLE II

## SEVERAL VALUES USED IN CALCULATION

Conductivity of Styrofoam Watt/(°Km)	Conductance of Woods <sub>2</sub> Watt/(°Km)	Thickness of Styrofoam m	Emissivity of Cover	Emissivity of Plate
0.036	1.817	0.051	0.63	0.96
Transmissivity of cover	Area of Plate m <sup>2</sup>	Area of Edge m <sup>2</sup>	Specific Heat of Water cal/(gr°K)	Stafan-Boltzmann Constant Watt/(°K <sup>4</sup> m <sup>2</sup> )
0.3	2.276	0.186	1.	5.670x10 <sup>-8</sup>

values of wind velocity depending on time were not available, for the first trial run test of the model, all the hourly wind velocities were assumed to be 3.12 m/sec. From the outputs, the calculated outlet water temperatures were in good agreement with actually measured outlet water temperatures except those for 9 o'clock p.m. and 7 o'clock a.m. On that night the test was started a little late because the thermocouple, which was inside the outlet water tube of the first section of the bare collectors, was faulty and was repaired. Even though the recorder was turned on at about 8 o'clock, the thermocouple indications were not stable at 9 o'clock. On the next day, the sun rose before 7 o'clock in the morning. But in the model, the sun energy input was not considered such that there was large temperature difference between actual and calculated outlet water temperature at 7 o'clock.

Wind velocity affects the outlet water temperature drop. From comparing the Equation (17) with the Equation (32) or Equation (33) it is evident that, the bare collectors are more sensitive to the wind velocity than are the covered collectors. On the bare collectors, when the energy loss rate through the top of collector,  $Q_T$ , is negative, that means the average plate temperature is lower than the ambient temperature, and, as the wind velocity becomes lower, the outlet water temperature will drop more because of a decreased value of top loss coefficient. Also, when  $Q_T$  is negative but the wind velocity becomes higher, the temperature will drop less. When the energy loss rate through the top of the collector,  $Q_T$ , is positive, which means the heat will flow from plate to ambient, and, as the wind velocity becomes lower, the outlet water temperature will drop less because of a decreased value of top loss coefficient. When  $Q_T$  is positive but the wind velocity becomes higher, the outlet water temperature will drop more. By using the above general ideas and examining the calculated results, the wind velocities were adjusted to be between 1.79 m/sec and 3.57



m/sec respectively on the second computational trial run to get the calculated outlet water temperatures closer to actual outlet water temperatures. The value of cloud cover and wind velocity used in the first trial run and the second trial run are shown in Table III. Figure 18 shows the graphical representation of the actual and the two calculated outlet water temperatures. All the calculated outlet water temperatures agreed well with the actual outlet water temperatures. As expected, at the bare collectors, the outlet water temperatures from the second trial run agreed better with the actual temperature than the first trial, and for the covered collectors there were small changes depending on changes in assumed wind velocities.













Appendix D is the computer output for the 2:00 a.m. hour values for all the data sets except three rainy nights and the 6 August data set. 6 August data set was analyzed and discussed in detail above and three rainy night data sets results agreed well with Brunt's cloud coverage Equation (2). The reason why the 2:00 a.m. data was used is that 2:00 a.m. was the mid-point of the tests and the temperature data were, in general, stable compared with other times. The inlet water temperatures, and flow rates are listed in the computer output. Each line of the computer output represents the computations for one section of each kind of collector. Thus there are four lines for each data set. The observed data of cloud coverage and wind velocity were used at the first computer trial run. From the computer output it is generally observed that the nocturnal sky radiation heat loss rate, QRPS, was the dominant part of total energy loss rate of both kinds of collectors. From Equation (10) and Equation (31), it can be seen that the tenths of cloud coverage has much effect on the value of the nocturnal sky radiation heat loss rate for both kinds of collectors. If the tenths of cloud coverage decreases, the nocturnal sky radiation loss will increased such that the outlet water temperature drops more, and conversely.

TABLE III  
INPUT DATA OF RUN-1 AND RUN-2 FOR 6 AUGUST 1977

Time		9	10	11	12	1	2	3	4	5	6	7
Computational RUN-1	Tenths of Cloud	0	0	0	0	0	0	0	0	0	0	0
	Wind Velocity (m/sec)	3.12	3.12	3.12	3.12	3.12	3.12	3.12	3.12	3.12	3.12	3.12
Computational RUN-2	Tenths of Cloud	0	0	0	0	0	0	0	0	0	0	0
	Wind Velocity (m/sec)	2.23	2.23	2.23	2.23	2.23	1.79	3.57	3.12	2.23	3.12	2.23



# LEGEND OF FIGURE 18

	Entering water temperature
	Ambient temperature
	Actual outlet water temperature at first section of bare collector
	Actual outlet water temperature at second section of bare collector
	Actual outlet water temperature at first section of covered collector
	Actual outlet water temperature at second section of covered collector
	First calculated outlet water temperature at first section of bare collector
	Second calculated outlet water temperature at first section of bare collector
	First calculated outlet water temperature at second section of bare collector
	Second calculated outlet water temperature at second section of bare collector
	First <u>and</u> second calculated outlet temperature at first section of covered collector
	First <u>and</u> second calculated outlet temperature at second section of covered collector

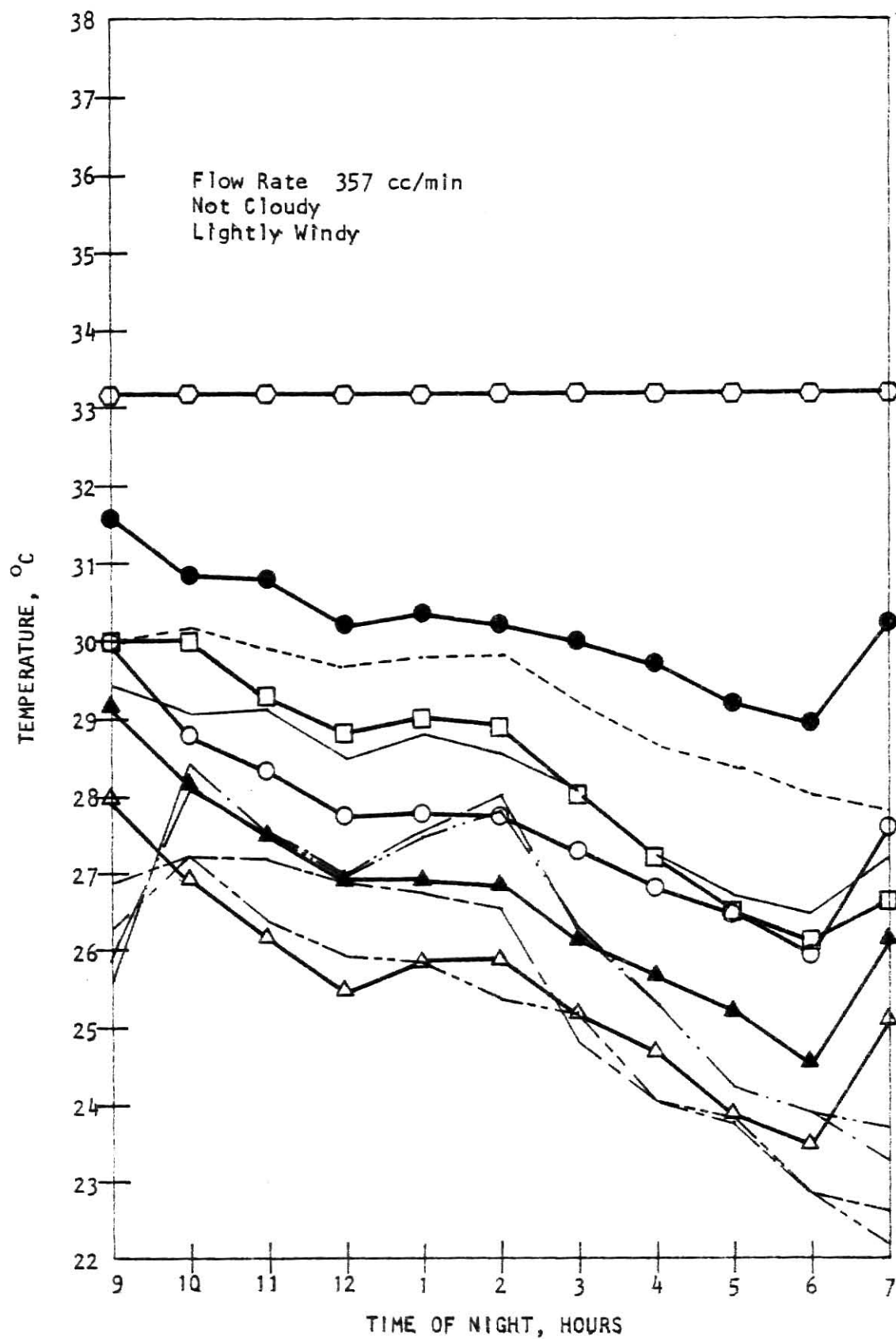


Figure 18. Comparison between Actual and Calculated Outlet Temperature

However, it was pointed out earlier that the determination of tenths of cloud coverage was uncertain. The tenths of cloud coverage also varied with time. Despite the uncertainties of tenths of cloud coverage and of wind velocities, the outputs of calculated outlet water temperatures agreed well with the actual outlet water temperatures.

The second and the third computer trial run were done to get the calculated outlet water temperatures closer to the actual outlet water temperatures. For the second trial computation only the values of cloud coverage were changed slightly, the changes based on the discussion above and examination of the results of the first trial computation. The changes of tenths of cloud coverage were listed in Table IV. From the output, it can be observed that the tenths of cloud coverage effected much the outlet water temperature for both kinds of collector. In this computer program, Equation (4) was used for the effect of cloud coverage instead of Equation (2) simply because Equation (4) was the result from U.S. as mentioned earlier.

Like the tenths of cloud coverage, the wind velocity is quite variable depending upon time. As previously discussed, the wind velocities were a little changed for the third trial computation. The values of the wind velocity used are also listed in Table IV. The calculated outlet water temperatures of third trial run agreed with the actual outlet water temperatures better than those of the first or the second trial run.

Based on the above discussion and an examination of the outputs of the computer program, the following observations may be made:

1. The tenths of cloud coverage, which should be defined clearly, strongly influenced the calculated outlet water-temperature for both kinds of collectors.

TABLE IV  
INPUT DATA OF RUN-1, RUN-2 AND RUN-3  
FOR 2 O'CLOCK EVERY DAY

The Number of Data Set	1	2	3	4	5	6	7	8	9	10	11
RUN - 1	Tenths of Cloud										
	10	8	0	2	6	0	8	8	8	2	0
RUN - 2	Wind Velocity (m/sec)										
	1.34	1.34	4.47	0.	4.02	1.78	0.	2.23	1.78	1.78	1.78
RUN - 3	Tenths of Cloud										
	10	9	0	0	6	2	10	10	10	0	0
RUN - 3	Wind Velocity (m/sec)										
	1.34	1.34	4.47	0.	4.02	1.78	0.	2.23	1.78	1.78	1.78
RUN - 3	Tenths of Cloud										
	10	9	0	0	6	2	10	10	10	0	0
RUN - 3	Wind Velocity (m/sec)										
	1.34	1.34	4.47	0.89	4.92	2.23	0.44	2.33	2.23	1.78	1.78

2. The calculated outlet water temperatures of the uncovered collectors were more sensitive to the wind velocity than that of the covered collectors.
3. The predicted outlet water temperatures agreed well with the measured outlet temperatures even though there were uncertainties of cloud coverage and wind velocity.



## CHAPTER VI

### SUMMARY, CONCLUSIONS, AND RECOMMENDATIONS

#### Summary and Conclusions

Measurements of water temperature drop were made between 9:00 p.m. and 7:00 a.m. from 1 August to 31 August 1977, with water flowing through tubes in two different kinds of collectors, glazed and unglazed. For the glazed collector, a single sheet of 1 mil Tedlar was used as the cover. The temperature of inlet water and the flow rate of water were controlled by a constant temperature circulator. The range of flow conditions covered in this investigation were:

1. Inlet water temperature, 31.9 - 38.6°C.
2. Water flow rate, 119 - 357 cc/min.

Based on the experimental work and the outlet water temperature predictor model derived herein, the following conclusions are drawn:

1. Even though the area of collectors of this study was more than adequate to cool the water, the outlet water temperature was limited to between 2°C and 6°C below the ambient temperature for both kinds of collectors.
2. The minimum outlet water temperature of both kinds of collector on rainy nights was the same or only a little lower than ambient temperature and then only if the collector area was adequate.
3. Compared with uncovered collector the Tedlar-covered collector is not a good radiator because of its opaqueness to the long wave length spectrum. In order to use a Tedlar-covered collector for nocturnal sky radiation, a slow flow rate (compared with a bare collector) is

recommended, depending on the inlet water temperature and night conditions.

4. The outlet water temperatures calculated from the model are in good agreement with the measured values.
5. Based on the model, the tenths of cloud coverage strongly influenced the outlet water temperature drop on both kinds of collectors, but the wind velocity strongly influenced only the bare collector water outlet temperature.

#### Recommendations for Further Studies

The comparison of an uncovered collector and a Tedlar-covered collector, and the analysis of two different kinds of collectors were done in this study. Data were taken at three water flow rates and at three inlet water temperatures. Based on the results, the following recommendations can be made for further studies:

1. The effect of cloud coverage on the nocturnal sky radiation should be studied on the basis of accurate definition of tenths of cloud coverage.
2. Additional similar studies using lower or higher flow rates and changing of the collector angle are needed. The objective of these studies would be to find optimal flow rate for the given collector area and a given angle.
3. It is also recommended to study further how to use the nocturnally chilled water for passive or active airconditioning system.

## SELECTED BIBLIOGRAPHY

1. Löf, George O. G., Cooling with Solar Energy. Proceeding of the World Symposium on Applied Solar Energy, Phoenix Arizona, Menlo Park, Calif, Stanford Research Institute (1955), pp. 185-187.
2. Bliss, Jr. Raymond W., Atmospheric Radiation Near the Surface of the Ground. Solar Energy, Vol. 5, No. 3, (1961), pp. 103-120.
3. Brunt, D., Notes on Radiation in the Atmosphere, Quart. J. Roy. Meteorol. Soc., 58, (1932) pp. 389-420.
4. Picha, K. G., and Villanueva, Jose., Nocturnal Radiation Measurements, Atlanta, Georgia. Solar Energy, Vol. VI, No. 4, Oct. - Dec. 1962 pp. 151-154.
5. Swinback, W. C., Long Wave Radiation from Clear Skies, Quart. J. Roy. Meteorol. Soc., 89 (1963) pp. 339-348.
6. Wexler, H., Observations of Nocturnal Radiation at Fairbanks, Alaska and Fargo, North Dakota. U.S. Weather Bureau, Government Printing Office, 1941.
7. Meinel, Aden B., and Meinel, Marjorie P., Radiative Cooling. Applied Solar Energy, Addison-Wesley Publishing Co. 1976 pp. 451-453.
8. Yellott, John I., Cooling by Nocturnal Radiation and Evaporation. Solar Energy Utilization for heating and cooling N.S.F. 74-41 pp 59.17-59.18.
9. Kreider, Jan F., and Kreith, Frank, Sky-Therm System. Solar Heating and Cooling, McGrawHill Co. pp. 179-180.
10. Thomason, H. E., Three Solar House. Solar Energy Vol. IV, No. 4, Oct. 1960, pp. 11.
11. Thomason, H. L., and Thomason, H. J. L., Solar Houses, Heating and Cooling Progress Report. Solar Energy Vol. 15, No. 1, May 1973, pp. 27.
12. Bliss, Jr. Raymond W., The Performance of an Experimental System Using Solar Energy from Heating, and Night Radiation for Cooling a Building. New Sources of Energy, Proceedings of the Conference, Rome, 21-31 August 1961, Vol. 5, pp. 148.
13. Niles, P. W. B., K. L. Haggard, and H. R. Hay, Nocturnal Cooling and Solar Heating with Water Ponds and Movable Insulation Paper #1, Symposium #12.
14. Patton Arthur R., Night Radiation. Solar Energy for Heating and Cooling of Buildings, 1975, pp. 31-32.

15. Yellott, John I., Solar Energy Technology Chapter in ASHRAE Handbook. Workshop Proceedings, Solar Cooling for Buildings, Los Angeles, California, NSF-RA-N-74-063, Feb. 6-8, 1974, pp. 4-10.
16. Hay, H. R., and Yellott, J. I., A Naturally Air Conditioned Building. Mech. Eng. Vol. 92, 1970, pp. 19-25.
17. Löff, George O. G., Proceedings of the Solar Heating and Cooling for Buildings Workshop. (Part I: Technical Sessions, March 21 and 22) Washington, D. C. NSF-RA-N-73-004, March 21-23, 1973, pp. 6-7.
18. Whillier, A., Plastic Covers for Solar Collectors Solar Energy, Vol. 7, No. 3, (1964) pp. 148-151.
19. Whillier, A., Performance of Black-Painted Solar Air Heaters of Conventional Design. Solar Energy, Vol. 8, No. 1, 1964, pp. 31-37.
20. Whillier, A., Effect of Materials and Construction Details on the Thermal Performance of Solar Water Heaters. Solar Energy, Vol. 9, No. 1, 1965, pp. 21-26.
21. Francis de Winter, Solar Energy and the Flat Plate Collector - an Annotated Bibliography ASHRAE 1975.
22. Technical Information Bulletin TD-5, E. I. Du Pont De Nemours & Co. Film Department Specialty Markets Division, Wilmington, Delaware 19898.
23. Whillier Austin, Design Factors Influencing Collectors Performance. Low Temperature Engineering Application of Solar Energy. Technical Committee on Solar Energy Utilization of the ASHRAE 1967, pp. 27-40.
24. Simril, V. L., and Curry, Barbara A., The Properties of Polyvinyl Fluoride film. Journal of Applied Polymer Science, Vol. IV, Issue No. 10, (1960) pp. 62-68.
25. Kalb, G., D. D. Coffman, T. A. Ford, and F. C. Johnson, Journal of Applied Polymer Science, 4, 55 (1960).
26. Hay, Harold R., The Solar Era. Mechanical Engineering, October 1972, pp. 24-29.
27. Duffie, John A., and William A. Beckman, Flat-Plate Collectors. Solar Energy Thermal Process, John Wiley and Sons, New York, (1974) pp. 120-177.
28. Hottel, H. C. and Whillier, A., Evaluation of Flat-Plate Collector Performance. Transaction of the Performance on the Use of Solar Energy, 2, Part I, 74, University of Arizona Press, 1958.
29. McAdams, W. C., Heat Transmission, 3rd Ed., New York, McGraw-Hill Co., Inc., 1954.

30. Tabor, H., Radiation, Convection, and Conduction Coefficients in Solar Collectors. Bull. Res. Coun. Israel, 6c. 155 (1958).
31. J. P. Holman, Radiation Heat Transfer. Heat Transfer, 3rd Ed., McGraw-Hill Book Company, (1972) pp. 235-298.
32. Handbook of Fundamentals, ASHRAE 1972, pp. 357-363.
33. Berry, F., E. Bollay, and N. Beers, Handbook of Meteorology. McGraw-Hill Book Co., Inc., New York, 1945, pp. 903.
34. George Shortlley and Dudley Williams, Elements of Physics. Fifth Edition Prentice-Hall, Inc. 1971, Appendix.
35. Sprague, C. H. & Nash, R. T., Estimating uncertainty for measurement of individual variables. Introduction to Engineering Experimentation, Department of Mechanical Engineering, Kansas State University, Manhattan, Kansas, January, 1971, pp. 76-78.

## APPENDIX A

## NOMENCLATURE

Symbol	Significance	Units
A	Area	Sq. meter
C	Specific heat capacity of water	Cal/gr °K
C <sub>e</sub>	Conductance of edge material	W/m <sup>2</sup> °K
e	Partial pressure of water vapor in atmosphere	Milibar
h	Film heat transfer coefficient	W/m <sup>2</sup> °K
k	Conductivity	W/m °K
m	Mass flow rate	gram/sec
N	Tenths of cloud coverage	dimensionless
q	Rate of energy per unit area	Watt/m <sup>2</sup>
Q	Rate of energy	Watt
T	Temperature	°K
U	Loss coefficient	W/m <sup>2</sup> °K
GREEK		
ε	Emissivity	dimensionless
σ	Stefan-Boltzmann constant	W/K <sup>4</sup> m <sup>2</sup>
ζ	Transmissivity	dimensionless
SUBSCRIPTS		
1	Referred to first from the bottom of collector	
2	Referred to second from the bottom of collector	
3	Referred to first from the top of collector	
4	Referred to second from the top of collector	
a	Any property of air	

## NOMENCLATURE (CONTINUED)

## SUBSCRIPTS

ap	Apparent
b	Bottom
c	Any property of cover or convection term
cs	Clear sky
c-s	Cover to sky
dp	dewpoint
e	Any property of edge
i	Inlet condition
l	Total loss from the collector
o	Outlet condition
p	Any property of plate
p-c	Plate to cover
p-s	Plate to sky
r	Radiation term
s	Any property of sky
t	Top
w	Water
wind	Wind
w-p	Water to plate

**APPENDIX B****COMPUTER PROGRAM**



```

$JOB
C
C      *      *      *      *      *      *      *      *      *      *      *      *      *
C      *      *      *      *      *      *      *      *      *      *      *      *      *
C
1      DIMENSION TEMPI(60),TEMPP1(60),TEMPP2(60),TEMPP3(60),TEMPA(60)
2      DIMENSION TEMPC(60),TEMPO(60),TEMPP(60),TEMPS(60),VEL(60),DM(60)
3      INTEGER COVER(60),CN(60)
4      REAL KS
C
C      *      *      *      *      *      *      *      *      *      *      *      *      *
C
C      INFORMATION CONTAINED IN INPUT DATA
C
C      COVER      = INTEGER USED TO DISTINGUISH COLLECTORS
C                  -1    COLLECTOR WITH COVER
C                  1    COLLECTOR WITHOUT COVER
C      CN          = TENTHS OF CLOUDS
C      VEL         = WIND VELOCITY ( METER/SEC )
C      DM          = MASS FLOW RATE ( GRAM/SEC )
C      TEMP        = TEMPERATURE ( KELVIN )
C                  TEMPI    INLET WATER TEMPERATURE
C                  TEMPP1   PLATE TEMPERATURE AT INLET
C                  TEMPP2   PLATE TEMPERATURE AT MIDDLE
C                  TEMPP3   PLATE TEMPERATURE AT OUTLET
C                  TEMPA    AMBIENT TEMPERATURE
C                  TEMPC    COVER TEMPERATURE
C                  TEMPO    OUTLET WATER TEMPERATURE
C      KS          = CONDUCTIVITY OF BOTTOM MATERIAL ( WATT/(KELVIN*METER))
C      CE          = CONDUCTANCE OF EDGE MATERIAL ( WATT/(KELVIN*METER**2) )
C      TS          = THICKNESS OF BOTTOM ( METER )
C      EPSC        = EMISSIVITY OF COVER
C      EPSP        = EMISSIVITY OF PLATE
C      TRAN        = TRANSMISSIVITY OF COVER
C      AREAP       = AREA OF PLATE
C      AREAE       = AREA OF EDGE
C      C           = SPECIFIC HEAT ( CAL/(GRAM*KELVIN) )
C      SIGMA       = STAFAN-BOLTZMANN CONSTANT ( WATT/(KELVIN**4*METER**2) )
C
5      N=44
6      READ (5,100) (COVER(I),I=1,N)
7      READ (5,100) (CN(I),I=1,N)
8      100 FORMAT (16I5)
C
9      READ (5,101) (VEL(I),I=1,N)
10     READ (5,101) (DM(I),I=1,N)
11     101 FORMAT (16F5.2)
C
12     READ (5,200) (TEMPI(I),I=1,N)
13     READ (5,200) (TEMPP1(I),I=1,N)
14     READ (5,200) (TEMPP2(I),I=1,N)
15     READ (5,200) (TEMPP3(I),I=1,N)
16     READ (5,200) (TEMPA(I),I=1,N)
17     READ (5,200) (TEMPC(I),I=1,N)
18     READ (5,200) (TEMPO(I),I=1,N)
19     200 FORMAT (16F5.1)
C
20     READ (5,300) KS,CE,TS,EPSC,EPSP,TRAN,AREAP,AREAE,C,SIGMA
21     300 FORMAT (9F5.1,E10.3)
C

```

```

C      *      *      *      *      *      *      *      *      *      *      *      *      *
C
22      WRITE (6,400)
23      400 FORMAT ('1'/////64X,'RUN-1'////)
C
24      WRITE (6,500)
25      500 FORMAT (13X,'COVER',2X,'FLCW',3X,'TEMP1',3X,'TEMPO',3X,'TEMPA',3X,
C      C'EMPP',3X,'EMPC',5X,'Q',7X,'QB',4X,'QEDGE',3X,'GRPS',6X,'QT',3X,
C      C'EMPC',3X,'EMPC'//)
C
C      *      *      *      *      *      *      *      *      *      *      *      *      *
C
C      INFORMATION CONTAINED IN MAIN PROGRAM
C
C      CHECK      = ABSCLUTE TEMPERATURE DIFFERENCE BETWEEN BEGINNING AND END
C                  OF ONE ITERATION
C      M          = DUMMY VARIABLE FOR RESTRICTION OF ITERATION
C      H          = HEAT TRANSFER CCEFFICIENT ( WATT/(METER**2*KELVIN) )
C      HPC        NATURAL CONVECTION HEAT TRANSFER CCEFFICIENT FROM
C                  PLATE TO COVER
C      HRPC       RADIATION HEAT TRANSFER COEFFICIENT FROM PLATE TO
C                  COVER
C      HRCS       RADIATION HEAT TRANSFER COEFFICIENT FROM COVER TO SKY
C      HW         FORCED CONVECTION HEAT TRANSFER COEFFICIENT FROM COVER
C                  TO AMBIENT
C      U          = HEAT TRANSFER CCEFFICIENT ( WATT/(METER**2*KELVIN) )
C      UB         TOTAL HEAT TRANSFER CCEFFICIENT THRUUGH BCTTOM OF
C                  COLLECTOR FROM PLATE TO AMBIENT
C      UT         TOTAL HEAT TRANSFER CCEFFICIENT THRUUGH TOP OF COLLECTOR
C                  FROM PLATE TO AMBIENT
C      UEDGE      TOTAL HEAT TRANSFER CCEFFICIENT THRUUGH EDGE OF COLLECTOR
C                  FROM PLATE TO AMBIENT
C      Q          = TCTAL ENERGY LOSS RATE CF COLLECTOR FROM PLATE TO AMBIENT
C                  ( WATT )
C      QRPS       ENERGY LOSS RATE BECAUSE OF NCCTURNAL SKY RADIATION
C      QB         ENERGY LOSS RATE THRUUGH BOTTOM OF COLLECTOR FROM PLATE
C                  TO AMBIENT
C      QT         ENERGY LOSS RATE THRUUGH TOP OF COLLECTOR FROM PLATE TO
C                  AMBIENT
C      QEDGE      ENERGY LCSS RATE THRUUGH EDGE CF COLLECTOR FROM PLATE TO
C                  AMBIENT
C      TEMP       = TEMPERATURE ( KELVIN )
C      TEMPP      MEAN PLATE TEMPERATURE
C      TEMPS      EFFECTIVE SKY TEMPERATURE
C      TEMPCC     CALCULATED COVER TEMPERATURE
C      TEMPOC     CALCULATED OUTLET WATER TEMPERATURE
C      TEMPD      TEMPERATURE DIFFERENCE BETWEEN ACTUAL AND CALCULATED
C                  OUTLET WATER TEMPERATURE
C
26      M=1
27      UB=KS/TS
C
28      DO 1000 I=1,N
C
29      TEMPP(I)=(TEMPP1(I)+TEMPP2(I)+TEMPP3(I))/3.
30      TEMPS(I)=0.0552*TEMPA(I)**1.5
31      IF(COVER(I))1,2,2
C
32      1 IF (TEMPA(I)-TEMPP(I))3,4,4
33      4 HPC=0.

```

```

34      GO TO 10
35      3 HPC=1.5774*(TEMPP(I)-TEMPC(I))**0.25
36      10 HRPC=SIGMA*(TEMPC(I)+TEMPP(I))^(TEMPC(I)**2+TEMPP(I)**2)/(1/EPSP+1
      C/EPSC-1)
37      M=M+1
38      HW=5.7+3.8*VEL(I)
39      HRCS=EPSC*SIGMA*(TEMPC(I)**4-TEMPS(I)**4)/(TEMPC(I)-TEMPA(I))
40      UT=1/(1/(HPC+HRPC)+1/(HW+HRCS))
41      TEMPCC=TEMPP(I)-UT*(TEMPP(I)-TEMPA(I))/(HPC+HRPC)
42      CHECK=ABS(TEMPCC-TEMPC(I))
43      IF (M-5)7,7,5
44      7 IF (CHECK-0.5)5,6,6
45      6 TEMPC(I)=TEMPCC
46      GO TO 1
47      5 QRPS=TRAN*EPSP*SIGMA*(1-0.06*CN(I))*(TEMPP(I)**4-TEMPS(I)**4)*AREA
      CP
48      UEDGE=AREAE*CE/AREAP
49      GO TO 20
      C
50      2 UT=5.7+3.8*VEL(I)
51      QRPS=EPSP*SIGMA*(1-0.06*CN(I))*(TEMPP(I)**4-TEMPS(I)**4)*AREAP
52      UEDGE=0.
      C
53      20 QB=UB*AREAP*(TEMPP(I)-TEMPA(I))
54      QT=UT*AREAP*(TEMPP(I)-TEMPA(I))
55      QEDGE=UEdge*AREAP*(TEMPP(I)-TEMPA(I))
56      Q=QB+QT+QRPS+QEDGE
      C
57      TEMPOC=TEMPI(I)-Q/(DM(I)*C*4.184)
58      TEMPD=TEMPC(I)-TEMPCC
      C
59      WRITE(6,600)COVER(I),DM(I),TEMPI(I),TEMPO(I),TEMPA(I),TEMPP(I),TEM
      CPC(I),Q,QB,QEDGE,QRPS,QT,TEMPCC,TEMPD
60      600 FORMAT(12X,I5,F7.2,12F8.1)
      C
61      1000 CONTINUE
      C
      C      *      *      *      *      *      *      *      *      *      *      *      *      *
      C
62      WRITE (6,700)
63      700 FORMAT('1')
      C
      C      *      *      *      *      *      *      *      *      *      *      *      *      *
      C      *      *      *      *      *      *      *      *      *      *      *      *      *
      C
64      STOP
65      END

```

\$ENTRY

## APPENDIX C

## ORIGINAL DATA AND CALCULATED RESULTS

## Explanation of Terminology Used in Computer Output

Term	Meaning
COVER	Integer used to distinguish collectors -1      Collector with cover 1      Collector without cover
FLOW	Mass flow rate (gram/sec)
TEMPI	Inlet water temperature ( $^{\circ}\text{K}$ )
TEMPO	Outlet water temperature
TEMPA	Ambient temperature
TEMPP	Mean plate temperature
TEMPC	Cover temperature
Q	Total energy loss rate of collector (watt)
QB	Energy loss rate through the bottom of collector
QEDGE	Energy loss rate through the edge of collector
QRPS	Energy loss rate because of nocturnal sky radiation
QT	Energy loss rate through the top of collector
TEMPOC	Calculated outlet water temperature ( $^{\circ}\text{K}$ )
TEMPOD	Temperature difference between actual and calculated outlet water temperature

## RUN-1

TIME	COVER	FLOW	TEMPI	TEMPO	TEMPA	TEMPP	TEMPC	Q	QB	QEDGE	QRPS	QT	TEMPOC	TEMPD
9	1	5.95	306.2	302.2	303.0	303.6	0.0	187.4	1.0	0.0	162.4	24.0	298.7	3.5
	1	5.95	302.2	301.0	303.0	301.3	0.0	58.4	-2.8	0.0	130.4	-69.3	299.9	1.1
	-1	5.95	306.2	304.6	303.0	304.9	303.5	80.4	3.0	0.6	54.0	22.7	303.0	1.6
10	-1	5.95	304.6	303.0	303.0	303.5	303.1	55.1	0.8	0.2	48.3	5.8	302.4	0.6
	1	5.95	306.2	301.2	303.0	302.4	0.0	122.8	-0.9	0.0	146.3	-22.7	301.3	-0.1
	1	5.95	301.2	300.0	303.0	300.2	0.0	1.5	-4.4	0.0	116.5	-110.6	301.1	-1.1
11	-1	5.95	306.2	303.9	303.0	304.6	303.5	74.5	2.5	0.5	52.8	18.7	303.2	0.7
	-1	5.95	303.9	301.8	303.0	302.9	302.5	45.2	-0.1	-0.0	46.0	-0.6	302.1	-0.3
	1	5.95	306.2	300.4	302.3	302.0	0.0	140.2	-0.5	0.0	152.7	-12.0	300.6	-0.2
12	1	5.95	300.4	299.2	302.3	299.5	0.0	4.4	-4.4	0.0	119.4	-110.6	300.2	-1.0
	-1	5.95	306.2	303.8	302.3	304.3	302.9	82.7	3.2	0.7	55.2	23.7	302.9	0.9
	-1	5.95	303.8	301.3	302.3	301.8	302.1	40.1	-0.7	-0.2	45.1	-4.2	302.2	-0.9
1	1	5.95	306.2	299.9	301.8	301.7	0.0	153.1	-0.2	0.0	157.3	-4.0	300.0	-0.1
	1	5.95	299.9	298.5	301.8	298.9	0.0	-0.8	-4.7	0.0	119.7	-115.9	299.9	-1.4
	-1	5.95	306.2	303.2	301.8	304.0	302.5	88.1	3.6	0.8	56.8	26.9	302.7	0.5
2	-1	5.95	303.2	300.7	301.8	301.4	301.7	41.7	-0.6	-0.1	46.0	-3.5	301.5	-0.8
	1	5.95	306.2	299.9	302.0	301.7	0.0	139.5	-0.5	0.0	153.4	-13.3	300.6	-0.7
	1	5.95	299.9	298.9	302.0	299.2	0.0	3.8	-4.5	0.0	120.2	-111.9	299.7	-0.8
3	-1	5.95	305.2	303.4	302.0	304.1	302.5	84.7	3.4	0.7	56.1	24.6	302.8	0.6
	-1	5.95	303.4	300.7	302.0	301.3	302.6	37.8	-1.1	-0.2	44.6	-5.6	301.9	-1.2
	1	5.95	306.2	299.8	301.9	301.4	0.0	128.9	-0.9	0.0	151.0	-21.3	301.0	-1.2
4	1	5.95	299.8	298.9	301.9	299.1	0.0	6.1	-4.4	0.0	121.1	-110.5	299.6	-0.7
	-1	5.95	306.2	303.2	301.5	303.9	302.3	85.0	3.3	0.7	55.9	25.1	302.8	0.4
	-1	5.95	303.2	300.7	301.9	301.4	301.6	40.0	-0.8	-0.2	45.4	-4.5	301.6	-0.9
5	1	5.95	306.2	299.1	301.0	301.2	0.0	170.7	0.3	0.0	163.8	6.7	299.3	-0.2
	1	5.95	299.1	298.2	301.0	298.7	0.0	33.4	-3.7	0.0	130.3	-93.2	297.8	0.4
	-1	5.95	306.2	303.0	301.0	303.8	302.0	55.6	4.6	1.0	60.1	33.9	302.2	0.8
6	-1	5.95	303.0	300.3	301.0	301.1	300.9	50.2	0.2	0.0	48.9	1.1	301.0	-0.7
	1	5.95	306.2	298.7	300.2	300.8	0.0	155.5	0.9	0.0	171.9	22.6	298.3	0.4
	1	5.95	298.7	297.7	300.2	298.0	0.0	41.9	-3.6	0.0	134.7	-89.2	297.0	0.7
7	-1	5.95	306.2	302.7	300.2	303.7	301.2	113.9	5.7	1.2	63.8	43.3	301.6	1.1
	-1	5.95	302.7	299.8	300.2	300.8	300.4	59.6	1.0	0.2	51.7	6.7	300.3	-0.5
	1	5.95	306.2	298.3	299.5	300.6	0.0	228.9	1.8	0.0	181.8	45.3	297.0	1.3
8	1	5.95	298.3	296.9	299.5	297.1	0.0	37.1	-3.8	0.0	135.5	-94.6	296.8	0.1
	-1	5.95	306.2	302.2	299.5	303.4	300.3	122.5	6.3	1.3	65.9	49.0	301.3	0.9
	-1	5.95	302.2	299.5	299.5	300.2	300.0	61.5	1.1	0.2	52.8	7.4	299.7	-0.2
9	1	5.95	306.2	297.6	299.1	300.3	0.0	233.8	1.9	0.0	184.0	47.9	296.8	0.8
	1	5.95	297.6	296.5	299.1	296.9	0.0	47.7	-3.5	0.0	139.1	52.7	295.7	0.8
	-1	5.95	306.2	302.0	299.1	303.3	299.3	62.5	1.1	0.2	53.2	7.9	299.5	-0.6
10	-1	5.95	302.0	298.9	299.1	299.8	299.3	248.8	2.4	0.0	186.5	59.9	296.2	2.9
	1	5.95	306.2	299.1	299.6	301.1	0.0	87.8	-2.3	0.0	147.4	-57.3	295.6	2.5
	-1	5.95	299.1	298.1	299.6	298.2	0.0	135.4	7.3	1.5	68.6	58.0	300.8	2.4
11	-1	5.95	306.2	303.2	299.6	304.2	300.5	75.3	2.3	0.5	55.7	16.9	300.2	0.3
	-1	5.95	303.2	300.5	299.6	301.0	300.0							
	-1	5.95	303.2	300.5	299.6	301.0	300.0							

## RUN-2

TIME	COVER	FLOW	TEMPI	TEMPO	TEMPA	TEMPP	TEMPC	C	QB	QEDGE	* QRPS	QT	TEMPDC	TEMPO
9	1	5.95	306.2	302.2	303.0	303.6	0.0	182.7	1.0	0.0	162.4	19.4	298.9	3.3
	1	5.95	302.2	301.0	303.0	301.3	0.0	71.7	-2.8	0.0	130.4	-55.9	299.3	1.7
	-1	5.95	306.2	304.6	303.0	304.9	303.5	80.4	3.0	0.6	54.0	22.7	303.0	1.6
10	-1	5.95	304.6	303.0	303.0	303.5	303.1	55.1	0.8	0.2	48.3	5.8	302.4	0.6
	1	5.95	306.2	301.2	303.0	302.4	0.0	127.1	-0.9	0.0	146.3	-18.3	301.1	0.1
	1	5.95	301.2	300.0	303.0	300.2	0.0	22.8	-4.4	0.0	116.5	-89.3	300.3	-0.3
11	-1	5.95	306.2	303.9	303.0	304.6	303.5	74.5	2.5	0.5	52.8	18.7	303.2	0.7
	-1	5.95	303.9	301.8	303.0	302.9	302.9	45.2	-0.1	-0.0	46.0	-0.6	302.1	-0.3
	1	5.95	306.2	300.4	302.3	302.0	0.0	142.5	-0.5	0.0	152.7	-9.7	300.5	-0.1
12	1	5.95	300.4	299.2	302.3	299.5	0.0	25.7	-4.4	0.0	119.4	-89.3	299.4	-0.2
	-1	5.95	306.2	303.8	302.3	304.3	302.9	82.7	3.2	0.7	55.2	23.7	302.9	0.9
	-1	5.95	303.8	301.3	302.3	301.8	302.1	40.1	-0.7	-0.2	45.1	-4.1	302.2	-0.9
1	1	5.95	306.2	299.9	301.8	301.7	0.0	153.9	-0.2	0.0	157.3	-3.2	300.0	-0.1
	1	5.95	299.9	298.5	301.8	298.9	0.0	21.5	-4.7	0.0	119.7	-93.6	299.0	-0.5
	-1	5.95	306.2	303.2	301.8	304.0	302.5	88.0	3.6	0.8	56.8	26.8	302.7	0.5
2	-1	5.95	303.2	300.7	301.8	301.4	301.7	41.7	-0.6	-0.1	46.0	-3.5	301.5	-0.8
	1	5.95	306.2	299.9	302.0	301.7	0.0	142.1	-0.5	0.0	153.4	-10.8	300.5	-0.6
	1	5.95	299.9	298.9	302.0	299.2	0.0	25.4	-4.5	0.0	120.2	-50.3	298.9	0.0
3	-1	5.95	306.2	303.4	302.0	304.1	302.9	84.7	3.4	0.7	56.1	24.5	302.8	0.6
	-1	5.95	303.4	300.7	302.0	301.3	302.6	37.8	-1.1	-0.2	44.6	-5.6	301.9	-1.2
	1	5.95	299.8	298.9	301.9	299.1	0.0	135.0	-0.9	0.0	151.0	-15.2	300.8	-1.0
4	-1	5.95	306.2	303.2	301.9	303.9	302.3	84.9	-4.4	0.0	121.1	-78.7	298.3	0.6
	-1	5.95	303.2	300.7	301.9	301.4	301.6	40.0	3.3	0.7	55.9	25.1	302.8	0.4
	1	5.95	306.2	299.1	301.0	301.2	0.0	171.3	-0.8	-0.2	45.4	-4.5	301.6	-0.9
5	-1	5.95	306.2	303.0	301.0	303.8	302.0	55.6	4.6	1.0	130.3	-102.3	298.1	0.1
	-1	5.95	303.0	300.3	301.0	301.1	300.9	50.2	-3.7	0.0	60.1	34.0	302.2	0.8
	1	5.95	306.2	298.7	300.2	300.8	0.0	195.5	0.2	0.0	48.9	1.1	301.0	-0.7
6	1	5.95	306.2	297.7	300.2	300.8	0.0	41.9	0.9	0.0	171.9	22.6	298.3	0.4
	-1	5.95	306.2	302.7	300.2	303.7	301.2	113.9	-3.6	0.0	134.7	-89.2	297.0	0.7
	-1	5.95	302.7	299.8	300.2	300.8	300.4	55.6	5.7	1.2	63.8	43.3	301.6	1.1
7	-1	5.95	306.2	298.3	299.5	303.4	300.3	122.3	6.3	0.2	51.7	6.7	300.3	-0.5
	1	5.95	306.2	296.9	299.5	300.6	0.0	220.2	1.8	0.0	181.8	36.6	297.4	0.9
	-1	5.95	302.2	299.5	299.5	300.2	300.0	55.4	-3.8	0.0	135.5	-76.3	296.1	0.8
8	-1	5.95	306.2	297.6	299.1	300.3	0.0	61.5	1.1	0.2	65.9	48.9	301.3	0.9
	1	5.95	306.2	296.5	299.1	296.9	0.0	233.8	1.9	0.0	52.8	7.4	299.7	-0.2
	-1	5.95	306.2	302.0	299.1	303.3	303.0	128.3	-3.5	1.4	67.5	52.7	301.0	1.0
9	-1	5.95	302.0	298.9	299.1	299.8	299.3	62.5	1.1	0.2	53.2	7.9	299.5	-0.6
	1	5.95	306.2	299.1	299.6	301.1	0.0	237.2	2.4	0.0	186.5	48.4	296.7	2.4
	-1	5.95	299.1	298.1	299.6	298.2	0.0	98.8	-2.3	0.0	147.4	-46.2	295.1	3.0
10	-1	5.95	306.2	303.2	299.6	304.2	300.5	135.2	7.3	1.5	68.6	57.8	300.8	2.4
	1	5.95	303.2	300.5	299.6	301.0	300.0	75.3	2.3	0.5	55.7	16.9	300.2	0.3
	-1	5.95	303.2	300.5	299.6	301.0	300.0	75.3	2.3	0.5	55.7	16.9	300.2	0.3

**APPENDIX D****ORIGINAL DATA AND CALCULATED RESULTS**

## RUN-1

DATA	COVER	FLOW	TEMPI	TEMPO	TEMPA	TEMPP	TEMPC	Q	QB	QEDGE	QRPS	QT	TEMPOC	TEMPOD
1	1	1.98	308.0	291.8	293.6	296.0	0.0	149.6	3.9	0.0	85.9	59.8	289.9	1.9
	1	1.98	291.8	291.0	293.6	291.5	0.0	9.2	-3.3	0.0	63.3	-50.8	290.7	0.3
	-1	1.98	308.0	293.7	293.6	299.1	294.2	112.0	8.8	1.9	30.6	70.8	294.5	-0.8
2	-1	1.98	293.7	292.7	293.6	292.4	293.3	7.8	-2.0	-0.4	20.2	-10.0	292.8	-0.1
	1	1.98	307.0	290.9	293.0	294.9	0.0	158.5	3.1	0.0	108.8	46.7	287.9	3.0
	1	1.98	290.9	290.0	293.0	290.6	0.0	19.3	-3.8	0.0	81.2	-58.1	288.6	1.4
3	-1	1.98	307.0	292.9	293.0	298.1	293.5	115.1	8.2	1.7	39.2	65.9	293.1	-0.2
	-1	1.98	292.9	291.0	293.0	291.6	293.1	12.0	-2.3	-0.5	26.1	-11.3	291.4	-0.4
	1	3.96	310.2	297.8	299.9	300.7	0.0	218.6	1.3	0.0	176.1	41.3	297.0	0.8
	1	3.96	297.8	297.3	299.5	297.5	0.0	8.0	-3.8	0.0	134.1	-122.2	297.3	-0.0
	-1	3.96	310.2	301.7	299.9	304.8	301.0	140.9	7.8	1.6	69.6	61.8	301.7	0.0
4	-1	3.96	301.7	298.9	299.9	299.7	299.8	46.2	-0.4	-0.1	48.7	-2.0	298.9	-0.0
	1	3.96	309.7	287.8	289.2	295.6	0.0	333.5	10.3	0.0	240.2	83.0	289.6	-1.8
	1	3.96	287.8	283.6	289.2	285.7	0.0	84.0	-5.6	0.0	134.5	-45.0	282.7	0.9
	-1	3.96	309.7	293.3	289.2	300.0	291.0	242.0	17.3	3.6	87.1	133.9	295.1	-1.8
5	-1	3.96	293.3	288.7	289.2	289.5	289.3	55.1	0.4	0.1	52.0	2.6	290.0	-1.3
	1	5.95	311.6	300.1	300.1	303.1	0.0	281.4	4.9	0.0	131.8	144.8	300.3	-0.2
	1	5.95	300.1	298.4	300.1	299.3	0.0	61.0	-1.2	0.0	98.8	-36.6	297.7	0.7
	-1	5.95	311.6	304.6	300.1	307.1	302.0	153.7	11.3	2.4	50.3	89.6	305.4	-0.8
6	-1	5.95	304.6	301.3	300.1	302.4	301.0	68.5	3.6	0.8	37.5	26.6	301.8	-0.5
	1	5.95	309.0	290.7	289.8	296.9	0.0	494.1	11.4	0.0	281.3	201.4	289.2	1.5
	1	5.95	290.7	287.2	289.8	308.4	0.0	132.3	-2.3	0.0	175.3	-40.7	285.4	1.8
	-1	5.95	309.0	297.9	289.8	302.2	294.0	277.1	19.9	4.2	105.6	147.4	297.9	0.0
7	-1	5.95	297.9	292.6	289.8	293.9	291.0	128.3	6.6	1.4	72.9	47.5	292.7	-0.1
	1	1.98	305.0	296.4	298.8	299.0	0.0	92.9	0.4	0.0	89.5	3.0	293.8	2.6
	1	1.98	296.4	295.8	298.8	296.1	0.0	29.5	-4.4	0.0	69.3	-35.5	292.8	3.0
	-1	1.98	305.0	298.7	298.8	300.6	299.2	55.7	2.9	0.6	30.2	22.0	298.3	0.4
8	-1	1.98	298.7	297.6	298.5	297.4	298.2	8.4	-2.2	-0.5	23.5	-12.4	297.7	-0.1
	1	1.98	304.5	296.8	298.5	298.4	0.0	85.6	-0.1	0.0	87.9	-2.2	294.6	2.2
	1	1.98	296.8	296.7	298.5	296.7	0.0	16.5	-2.8	0.0	76.3	-57.0	294.8	1.9
	-1	1.98	304.9	297.9	298.5	300.5	299.0	55.0	3.3	0.7	30.7	24.3	297.8	0.1
	-1	1.98	297.9	296.8	298.5	297.2	298.0	9.5	-2.1	-0.5	23.8	-11.7	296.8	0.0
9	1	3.96	305.8	295.1	295.2	298.4	0.0	212.1	5.2	0.0	115.2	91.7	293.0	2.1
	1	3.96	295.1	293.5	295.2	294.3	0.0	59.3	-1.5	0.0	87.2	-26.5	291.5	2.0
	-1	3.96	305.8	298.5	295.2	301.4	297.0	127.6	10.0	2.1	40.7	74.8	298.1	0.4
10	-1	3.96	298.5	295.9	295.2	296.5	295.6	47.3	2.0	0.4	30.6	14.3	295.6	0.3
	1	3.96	305.6	298.8	301.6	300.5	0.0	92.8	-1.8	0.0	126.8	-32.2	300.0	-1.2
	1	3.96	298.8	298.0	301.6	298.3	0.0	2.5	-5.3	0.0	101.4	-93.6	298.7	-0.7
	-1	3.96	305.6	301.8	301.6	302.7	302.0	61.5	1.8	0.4	46.2	13.2	301.9	-0.1
11	-1	3.96	301.8	299.9	301.6	299.8	300.2	12.8	-2.8	-0.6	35.8	-19.6	301.0	0.4
	1	5.95	306.8	294.8	296.0	299.1	0.0	309.4	4.9	0.0	217.4	87.0	294.4	0.7
	1	5.95	294.8	292.7	296.0	293.5	0.0	70.7	-4.0	0.0	145.7	-70.9	292.0	0.7
	-1	5.95	306.8	299.7	296.0	302.4	299.0	164.4	10.3	2.2	78.7	73.3	300.2	-0.5
	-1	5.95	299.7	296.0	296.0	297.3	296.3	75.2	2.0	0.4	58.1	14.6	296.7	-0.7



## RUN-2

DATA	COVER	FLOW	TEMPI	TEMPO	TEMPA	TEMPP	TEMPC	C	QB	QEDGE	QRPS	QT	TEMPOC	TEMPOD
1	1	1.98	308.0	291.8	293.6	296.0	0.0	145.6	3.9	0.0	85.9	59.8	289.9	1.9
	1	1.98	291.8	291.0	293.6	291.5	0.0	9.2	-3.3	0.0	63.3	-50.8	290.7	0.3
	-1	1.98	308.0	293.7	293.6	299.1	294.2	112.0	8.8	1.9	30.6	70.8	294.5	-0.8
2	-1	1.98	293.7	292.7	293.6	292.4	293.3	7.8	-2.0	-0.4	20.2	-10.0	292.8	-0.1
	1	1.98	307.0	290.9	293.6	294.9	0.0	146.0	3.1	0.0	96.2	46.7	289.4	1.5
	1	1.98	290.9	290.0	293.0	290.6	0.0	9.9	-3.8	0.0	71.8	-58.1	289.7	0.3
3	-1	1.98	307.0	292.9	293.0	298.1	293.5	110.5	8.2	1.7	34.6	65.9	293.7	-0.8
	-1	1.98	292.9	291.0	293.0	291.6	293.1	9.0	-2.3	-0.5	23.1	-11.3	291.8	-0.8
	1	3.96	310.2	297.8	299.9	300.7	0.0	218.6	1.3	0.0	176.1	41.3	297.0	0.8
4	1	3.96	310.2	301.7	299.9	304.8	301.0	140.9	7.8	1.6	69.6	61.8	301.7	0.0
	-1	3.96	301.7	298.9	299.5	299.7	299.8	46.2	-0.4	-0.1	48.7	-2.0	298.9	-0.0
	1	3.96	309.7	287.8	289.2	295.6	0.0	366.3	10.3	0.0	273.0	83.0	287.6	0.2
5	1	3.96	309.7	283.6	289.2	285.7	0.0	102.3	-5.6	0.0	152.9	-45.0	281.6	2.0
	-1	3.96	309.7	293.3	289.2	300.0	291.0	253.8	17.3	3.6	99.0	133.9	294.4	-1.1
	-1	5.95	311.6	300.1	300.1	303.1	289.3	62.2	0.4	0.1	59.1	2.6	289.5	-0.8
6	1	5.95	300.1	298.4	300.1	299.3	0.0	281.4	4.9	0.0	131.8	144.8	300.3	-0.2
	-1	5.95	311.6	304.6	300.1	307.1	302.0	153.7	11.3	2.4	50.3	-36.6	297.7	0.7
	-1	5.95	304.6	301.3	300.1	302.4	301.0	68.5	3.6	0.8	37.5	26.6	305.4	-0.8
7	1	5.95	309.0	290.7	289.8	296.9	0.0	460.4	11.4	0.0	247.5	201.4	290.5	-0.5
	-1	5.95	290.7	287.2	289.8	288.4	0.0	111.3	-2.3	0.0	154.3	-40.7	286.2	1.0
	-1	5.95	309.0	297.9	289.8	302.2	294.0	264.4	19.9	4.2	92.9	147.4	298.4	-0.5
8	-1	5.95	297.9	292.6	289.8	293.9	291.0	119.6	6.6	1.4	64.1	47.5	293.1	-0.5
	1	1.98	305.0	296.4	298.8	299.0	0.0	72.2	0.4	0.0	68.8	3.0	296.3	0.1
	1	1.98	296.4	295.8	298.8	296.1	0.0	13.5	-4.4	0.0	53.3	-35.5	294.8	1.0
9	-1	1.98	305.0	298.7	298.8	300.6	299.2	48.7	2.9	0.6	23.2	22.0	295.1	-0.4
	-1	1.98	298.7	297.6	298.8	297.4	298.2	3.0	-2.2	-0.5	18.1	-12.4	298.3	-0.7
	1	1.98	304.9	296.8	298.5	298.4	0.0	65.3	-0.1	0.0	67.6	-57.0	297.0	-0.2
10	-1	1.98	304.9	297.9	298.5	300.5	299.0	51.9	3.3	0.7	58.7	24.3	296.9	-0.7
	-1	1.98	297.9	296.8	298.5	297.2	298.0	4.0	-2.1	-0.5	23.6	-11.7	297.4	-0.6
	1	3.96	305.8	295.1	295.2	298.4	0.0	185.5	5.2	0.0	88.6	91.7	294.6	0.5
11	1	3.96	295.1	293.5	295.2	294.3	0.0	39.1	-1.5	0.0	67.1	-26.5	292.7	0.8
	-1	3.96	305.8	298.5	295.2	301.4	297.0	118.2	10.0	2.1	31.3	74.8	298.7	-0.2
	-1	3.96	298.5	295.9	295.2	296.5	295.6	40.3	2.0	0.4	23.5	14.3	296.1	-0.2
12	1	3.96	305.6	298.8	301.6	300.5	0.0	110.1	-1.8	0.0	144.0	-32.2	299.0	-0.2
	1	3.96	298.8	298.0	301.6	298.3	0.0	16.3	-5.3	0.0	115.2	-93.6	297.8	0.2
	-1	3.96	305.6	301.8	301.6	302.7	302.0	67.8	1.8	0.4	52.5	13.2	301.5	0.3
13	-1	3.96	301.8	299.9	301.6	299.8	300.2	17.6	-2.8	-0.6	40.7	-19.6	300.7	-0.8
	1	5.95	306.8	294.8	296.0	299.1	0.0	305.4	4.9	0.0	217.4	87.0	294.4	0.4
	1	5.95	294.8	292.7	296.0	293.5	0.0	70.7	-4.0	0.0	145.7	-70.9	292.0	0.7
14	-1	5.95	306.8	299.7	296.0	302.4	299.0	164.4	10.3	2.2	78.7	73.3	300.2	-0.5
	-1	5.95	299.7	296.0	296.0	297.3	296.3	75.2	2.0	0.4	58.1	14.6	296.7	-0.7
	-1	5.95	299.7	296.0	296.0	297.3	296.3	75.2	2.0	0.4	58.1	14.6	296.7	-0.7

## RUN-3

DATA	COVER	FLOW	TEMPI	TEMPC	TEMPA	TEMPP	TEMPC	Q	QB	QEDGE	QRPS	QT	TEMPOC	TEMPD
1	1	1.98	308.0	291.8	293.6	296.0	0.0	145.6	3.9	0.0	85.9	59.8	289.9	1.9
	1	1.98	291.8	291.0	293.6	291.5	0.0	9.2	-3.3	0.0	63.3	-50.8	290.7	0.3
	-1	1.98	308.0	293.7	293.6	299.1	294.2	112.0	8.8	1.9	30.6	70.8	294.5	-0.8
2	-1	1.98	293.7	292.7	293.6	292.4	293.3	7.8	-2.0	-0.4	20.2	-10.0	292.8	-0.1
	1	1.98	307.0	290.9	293.0	294.9	0.0	146.0	3.1	0.0	96.2	46.7	289.4	1.5
	1	1.98	290.9	290.0	293.0	290.6	0.0	9.9	-3.8	0.0	71.8	-58.1	289.7	0.3
3	-1	1.98	307.0	292.9	293.0	298.1	293.5	110.5	8.2	1.7	34.6	65.9	293.7	-0.8
	-1	1.98	292.9	291.0	293.0	291.6	293.1	9.0	-2.3	-0.5	23.1	-11.3	291.8	-0.8
	1	3.96	310.2	297.8	299.9	300.7	0.0	218.6	1.3	0.0	176.1	41.3	297.0	0.8
	1	3.96	297.8	297.3	299.9	297.5	0.0	8.0	-3.8	0.0	134.1	-122.2	297.3	-0.0
4	-1	3.96	310.2	301.7	299.9	304.8	301.0	140.9	7.8	1.6	69.6	61.8	301.7	0.0
	-1	3.96	301.7	298.9	299.9	299.7	299.8	46.2	-0.4	-0.1	48.7	-2.0	298.9	-0.0
	1	3.96	309.7	287.8	289.2	295.6	0.0	415.5	10.3	0.0	273.0	132.3	284.6	3.2
	1	3.96	287.8	283.6	289.2	285.7	0.0	75.6	-5.6	0.0	152.9	-71.7	283.2	0.4
5	-1	3.96	309.7	293.3	289.2	300.0	291.0	255.3	17.3	3.6	99.0	135.3	294.3	-1.0
	-1	3.96	293.3	288.7	289.2	289.5	289.3	62.2	0.4	0.1	59.1	2.6	289.5	-0.8
	1	5.95	311.6	300.1	300.1	303.1	0.0	305.1	4.9	0.0	131.8	168.4	299.3	0.8
	1	5.95	300.1	298.4	300.1	299.3	0.0	55.0	-1.2	0.0	98.8	-42.6	297.9	0.5
6	-1	5.95	311.6	304.6	300.1	307.1	302.0	154.3	11.3	2.4	50.3	90.3	305.4	-0.8
	-1	5.95	304.6	301.3	300.1	302.4	301.0	68.6	3.6	0.8	37.5	26.7	301.8	-0.5
	1	5.95	309.0	290.7	289.8	296.9	0.0	488.0	11.4	0.0	247.5	229.0	289.4	1.3
	1	5.95	290.7	287.2	289.8	288.4	0.0	105.7	-2.3	0.0	154.3	-46.2	286.5	0.7
	-1	5.95	309.0	297.9	289.8	302.2	294.0	265.9	19.9	4.2	92.9	148.9	298.3	-0.4
7	-1	5.95	297.9	292.6	289.8	293.9	291.0	115.7	6.6	1.4	64.1	47.6	293.1	-0.5
	1	1.98	305.0	296.4	298.8	299.0	0.0	73.1	0.4	0.0	68.8	3.9	296.2	0.2
	1	1.98	296.4	295.8	298.8	296.1	0.0	3.1	-4.4	0.0	53.3	-45.9	296.0	-0.2
	-1	1.98	305.0	298.7	298.8	300.6	299.2	48.7	2.9	0.6	23.2	22.0	299.1	-0.4
8	-1	1.98	298.7	297.6	298.8	297.4	298.2	3.0	-2.2	-0.5	18.1	-12.4	298.3	-0.7
	1	1.98	304.9	296.8	298.5	298.4	0.0	65.3	-0.1	0.0	67.6	-2.2	297.0	-0.2
	1	1.98	296.8	296.7	298.5	296.7	0.0	-2.6	-2.8	0.0	58.7	-58.5	297.1	-0.4
	-1	1.98	304.9	297.9	298.5	300.5	299.0	51.9	3.3	0.7	23.6	24.3	298.6	-0.7
9	-1	1.98	297.9	296.8	298.5	297.2	298.0	4.0	-2.1	-0.5	18.3	-11.7	297.4	-0.6
	1	3.96	305.8	295.1	295.2	298.4	0.0	198.1	5.2	0.0	88.6	104.3	293.8	1.3
	1	3.96	295.1	293.5	295.2	294.3	0.0	35.5	-1.5	0.0	67.1	-30.1	293.0	0.5
	-1	3.96	305.8	298.5	295.2	301.4	297.0	118.6	10.0	2.1	31.3	75.2	298.6	-0.1
10	-1	3.96	293.5	295.9	295.2	296.5	295.6	40.3	2.0	0.4	23.5	14.3	296.1	-0.2
	1	3.96	305.6	298.8	301.6	300.5	0.0	110.1	-1.8	0.0	144.0	-32.2	299.0	-0.2
	1	3.96	298.8	298.0	301.6	298.3	0.0	16.3	-5.3	0.0	115.2	-93.6	297.8	0.2
	-1	3.96	305.6	301.8	301.6	302.7	302.0	67.8	1.8	0.4	52.5	13.2	301.5	0.3
11	-1	3.96	301.8	299.9	301.6	299.8	300.2	17.6	-2.8	-0.6	40.7	-19.6	300.7	-0.8
	1	5.95	306.8	294.8	296.0	299.1	0.0	309.4	4.9	0.0	217.4	87.0	294.4	0.4
	1	5.95	294.8	292.7	296.0	293.5	0.0	70.7	-4.0	0.0	145.7	-70.9	292.0	0.7
	-1	5.95	306.8	299.7	296.0	302.4	299.0	164.4	10.3	2.2	78.7	73.3	300.2	-0.5
	-1	5.95	299.7	296.0	296.0	297.3	296.3	75.2	2.0	0.4	58.1	14.6	296.7	-0.7

## APPENDIX E

## ERROR AND UNCERTAINTY ESTIMATION

Sprague and Nash (35) have suggested equations to calculate the uncertainty in the measured system. For a general case in which a result is given as a function of various independently measure variables

$$H = f(z_1, z_2, \dots, z_n), \quad (35)$$

the uncertainty in the result is given by

$$\lambda_H = \sqrt{\sum_{i=1}^n (S_i \lambda_i)^2} \quad (36)$$

where  $\lambda_i$  is the uncertainty in the i'th measured value, and  $S_i$  is the sensitivity factor, defined as

$$S_i = \frac{\partial f}{\partial z_i} \frac{z}{f(z_1, z_2, \dots, z_n)} \quad (37)$$

If a portion of the measured values are not independent, then the equation of uncertainty is:

$$\lambda_H = \sqrt{\left[ \sum_{i=1}^k (S_i \lambda_i)^2 \right] + \sum_{j=k+1}^n (S_j \lambda_j)^2} \quad (38)$$

where values 1 through k are dependent measurements and values k+1 through n are independent measurements.

From the above equations, the uncertainties of temperature, and flow rate were calculated. The smallest measured values were used for these calculations to find the largest uncertainties encountered.

### Temperature

The uncertainties of the recorded temperatures are composed of the uncertainty in temperature sensed by the thermocouple, the uncertainty in the poten-

tiometer and recorder, and the resolution uncertainty. The estimated uncertainty of thermocouple temperature is  $\pm 1^{\circ}\text{C}$  from the calibration results of thermocouples. The uncertainty of reading the temperature is  $\pm \frac{1}{4}^{\circ}\text{C}$  from the manufacturer's literature. The resolution uncertainty is assumed 0.0125 mv, equal to 1/2 of the smallest scale division of strip chart paper. The smallest measured value of temperature was  $11^{\circ}\text{C}$  equal to 0.429 mv in potentiometer reading. All the sensitivities are 1. These uncertainties are all independent so Equation (36, 37) can be used for the calculation of the overall uncertainty. The root mean square value of the uncertainty in recorded temperatures is

$$\lambda_T = \sqrt{(\lambda_{\text{thermocouple}})^2 + (\lambda_{\text{linearity}})^2 + (\lambda_{\text{resolution}})^2}$$

$$\lambda_T = \sqrt{\left(\frac{1}{11}\right)^2 + \left(\frac{0.25}{11}\right)^2 + \left(\frac{0.0125}{0.429}\right)^2} = 9.8\%$$

#### Flow Rate

The uncertainties of flow rate are composed of the uncertainty of linearity and that of the resolution. The uncertainty of linearity for the flow meter is not available, so this value is assumed to be 5.95 cc/min, equal to 1/2 of the smallest scale division of the flow meter. The resolution uncertainty will be same as the value of linearity uncertainty. The sensitivities of all the performance parameters are 1. The smallest flow rate is 119 cc/min. All the components are independent of each other. From the above informations the overall uncertainty of flow rate reading at the worst case is

$$\lambda_F = \sqrt{(\lambda_{\text{linearity}})^2 + (\lambda_{\text{resolution}})^2}$$

$$\lambda_F = \sqrt{\left(\frac{5.95}{119}\right)^2 + \left(\frac{5.95}{119}\right)^2} = 7\%$$

## ACKNOWLEDGEMENT

I would like to express my sincere appreciation to my major advisor, Dr. H. D. Ball, for his direction, and consultation during this investigation.

Dr. R. B. Haytor suggested the problem and provided initial guidance. Dr. P. L. Miller was a constant source of financial aid during this study. Mr. R. D. Drumn helped in the construction of the apparatus. To all those who gave aid, I also would like to express my gratitude and thanks.

Special thanks are extended to my wife for typing the thesis and the willing sacrifice during my graduate study.

## VITA

Do-Young Han was born at Suwon, Kyungkido, Korea, on Feb. 2, 1949.

The first son and second child of Chung-Hee and Sung-Kum Han. He graduated from Young San High School in 1967, was awarded the B.S. degree in Mechanical Engineering in 1972 from the Seoul National University in Seoul, Korea. After serving military service for two and half years as a first lieutenant and working in an institute for one and half years, he came into the United States in the spring of 1976, and studied for his M.S. degree.

COMPARISON OF A COVERED COLLECTOR  
TO AN UNCOVERED COLLECTOR FOR NOCTURNAL  
SKY RADIATION

by

DO-YOUNG HAN

B.S., Seoul National University, Seoul, Korea, 1972

---

AN ABSTRACT OF A MASTER'S THESIS

Submitted in partial fulfillment of the  
requirements for the degree

MASTER OF SCIENCE

Department of Mechanical Engineering

KANSAS STATE UNIVERSITY

Manhattan, Kansas

1977

## ABSTRACT

The purpose of this study was to compare a Tedlar covered collector with an uncovered collector when used for nocturnal sky radiation. The modeling and the experimental work were made. The model was computed by a computer program. The experiments were taken between 9:00 p.m. and 7:00 a.m. from 1 August to 31 August 1977 for different flow rates and inlet water temperatures. The performance parameters were measured with water flowing through tubes in two different kinds of collectors, which were composed of two sections. During the test, the flow rate and the inlet water temperature were the same in both kinds of collectors.

The calculated outlet temperatures were in good agreement with the measured value. The water temperature drops for both kinds of collectors were limited, even though the area of collectors was more than adequate to cool the water. A slower flow rate, compared with that of the uncovered collector, was recommended to use the Tedlar-covered collector for nocturnal sky radiation because the Tedlar-covered collector was a poor radiator.